TEMPERATURE DEPENDENCE OF THE DAMPING CONSTANT (LINEWIDTH) OF RAMAN MODES IN $NaNO_2$ AND $(NH_4)_2SO_4$ NEAR THE PHASE TRANSITIONS.

by

ALİ KİRACI

THESIS SUBMITIED TO
THE GRADUATE SCHOOL OF NATURAL AND APPLIED SCIENCES
OF
THE ABANT İZZET BAYSAL UNIVERSITY
IN PARTIAL FULFILLMENT OF THE REQUIREMENTS FOR THE DEGREE
OF
MASTER OF SCIENCE
IN
THE DEPARTMENT OF PHYSICS

JUNE 2008

Approval of the Graduate School of Natural and Applied Science

Prof. Dr. Nihat ÇELEBİ

Director

I certify that this thesis satisfies all the requirements as a thesis for the degree of Master of Science.

Prof. Dr. Ahmet Turan ALAN

Head of Department

This is to certify that we have read this thesis and that in our opinion it is fully adequate, in scope and quality as a thesis for the degree of Master of Science.

Assist. Prof. Dr. Hüseyin KARAÇALI

Supervisor

Examining Committee Members

1. Prof. Dr. Hamit YURTSEVEN .....

2. Assoc. Prof. Dr. Ahmet VARİLCİ .....

3. Assist. Prof. Dr. Hüseyin KARAÇALI

ABSTRACT

TEMPERATURE DEPENDENCE OF THE DAMPING CONSTANT (LINEWIDTH) OF RAMAN MODES IN NaNO2 AND $(NH4)_2SO4$ NEAR THE PHASE TRANSITIONS.

Kiracı, Ali

Master of Science, Depertment of Physics
Supervisor: Assistant Prof. Dr. Hüseyin Karaçalı

June 2008, 82 pages

In this study, we analyzed the temperature dependence of the order parameter, damping constant and the activation energy in a wide range of temperatures for the $NaNO_2$ modes (B_1 asymmetric, B_2 libration, B_1 libration and A_2 libration) and $(NH_4)_2SO_4$ modes (υ_1, 364 cm^{-1} libration, 394 cm^{-1} libration). We used the order parameter equation predicted from the molecular field theory to calculate the order parameters in $NaNO_2$ and $(NH_4)_2SO_4$. By using these calculated values of the order parameter, we computed the damping constants for the modes of $NaNO_2$ and $(NH_4)_2SO_4$studied here. We related the theoretical values of damping constants to the experimental results. By using the calculated damping constants in the Arrhenius plots ($\ln\Gamma$ versus $\frac{1}{T}$), we determined the activation energy values of all modes of both $NaNO_2$ and $(NH_4)_2SO_4$ in different temperature ranges.

Keywords: Order Parameter, Damping Constant, Activation Energy, Sodyum Nitrite, Ammonium Sulfate.

ÖZET

SODYUM NİTRİT ($NaNO_2$) VE AMONYUM SÜLFATIN ($(NH_4)_2SO_4$) RAMAN KİPLERİ İÇİN SÖNÜM KATSAYILARININ FAZ GEÇİŞLERİ YAKINLARINDA SICAKLIĞA BAĞIMLILIĞI

Kiracı, Ali
Yüksek Lisans, Fizik Bölümü
Tez Danışman: Yrd. Doç. Dr. Hüseyin Karaçalı

Haziran 2008, 82 sayfa

Bu çalışmada sodyum nitrit,$NaNO_2$' ün, kipleri (B_1 asimetrik, B_2 dönmesel. B_1 dönmesel, ve A_2 dönmesel), amonyum sülftatın ,$(NH_4)_2SO_4$ kipleri (υ_1, 364 cm^{-1} dönmesel, ve 394 cm^{-1} dönmesel), için düzen parametereleri, sönüm katsayıları ve aktivasyon enerjilerinin sıcaklığa bağımlılığını geniş bir sıcaklık aralığı boyunca analiz ettik. Ortalama alan teorisinin öngördüğü düzen parametresi bağıntısından düzen parametrelerini sodyum nitrit ve amonyum sülfat için hesapladık. Hesapladığımız bu düzen parametre değerlerini kullanarak sönüm katsayısını hespladık ve hesapladığımız bu sönüm katsayısını deneysel sonuçlarla ilişkilendirdik. Son olarak, hesaplanan bu sönüm katsayısını kullanarak Arrhenius grafiklerini ($\ln\Gamma$ versus $\frac{1}{T}$) çizdik. Çizilen bu grafiklerin eğimlerinden yaralanarak sodyum nitrit ve amonyum sülfattaki çalışılan kiplerin farklı sıcaklık değerleri arasındaki aktivasyon enerji değelerini hesapladık.

Anahtar Kelimeler: Düzen Parametresi, Sönümlenme Katsayısı, Aktivasyon Enerjisi, Sodyum Nitrit, Amonyum Sülfat.

To My Family…...

ACKNOWLEDGMENTS

It is great pleasure to thank the many people who have contributed to the completion of this thesis. First of all, I would like to thank my thesis supervisor; Asist. Prof. Dr. Hüseyin KARAÇALI, for many discussions, guidance, support, his assistances and enlightening comments on my work. I would like to special thanks to Prof. Dr. Hamit YURTSEVEN for support and guidance.

I would like to thank my parents, my sisters for their continous supports, patience and encouragements which made me possible to continue my researches.

TABLE OF CONTENTS

LIST OF TABLES

TABLE

.

LIST OF FIGURES

FIGURES

INTRODUCTION

1.1 Phase Transitions

"A state of matter" is one of the many ways that matter can interact with itself to form a macroscopic homogenous phase. Substances generally have three states which are solid, liquid, and gas. There is also a fourth state of matter called as plasma (an ionized gas). Plasma state can be obtained by electric discharges in gases at temperatures from several thousands to several million Kelvins. So, it is impossible to observe a plasma state in current conditions on Earth. Plasmas are found in the stars (Papon *et al.* 2001). The states of matter (solid, liquid, gas) vary in density, mechanical properties, optical properties, etc. It is possible to observe a lot of different arrengament of atoms, molecules, or particles, for the same solid or liquid matter called phases. Experiments have shown changes of states or phase transitions. Phase transitions are manifested by the appearence of new properties of matter.

It is very diffucult to solve a many- body system exactly except for exteremly simple cases, for example 1-D Ising model. The diffuculty, in general, is to compute the partition function of a system, then writing down the interaction terms in the Hamiltonian and summing over all states. In Moleculer Field Theory (MFT), it is easier to solve a many-body problem by replacing all interactions with an avarage or effective interaction. By using MFT, one can reduce any multi-body problem into an

effective one-body problem. In the next chapter of this study the calculation of the order parameter will be computed by using the MFT.

When a phase transition occurs in a substance, the symmetry is broken. Symmetry plays an important role in studying of the phase transitions and critical phenomena. Landau proposed a parameter called “order parameter”, which is related to the broken symmetry. An order parameter is a physical quantity that indicates the degree of order of a system. It is the magnetization for the magnetic case and the density for the solid/liquid or liquid/gas transitions. The order parameter can take any value from 0 to 1. An order parameter of 0 indicates disordered or the most symmetric phase while an order parameter of 1 indicates ordered or the least symmetric phase. The qualitative meaning of this point of view (the value 0 corresponds to disordered and the value 1 corresponds to ordered phase) is that when the temperature decreases, the order of the system increases. For example, if one cooles down a liquid, after the solidification point is reached, it solidifies and we know that the crystalline solid is more ordered than the liquid. Another reason for this issue is that when a ferromagnetic material is cooled below its Curie point (the temperature above which it loses its ferromagnetic ability) the magnetic order in the system increases. At this point macroscopic magnetization appears and this is the evidence of the existence of magnetic order. The choice of the order parameter is not always very clear in some cases. For example, in the case of superconductivity the order parameter is the electrons associated with superconductivity and in the case of superfluidity the order parameter is the wave function of the superfluid phase (Papon *et al.* 2001).

The linewidth (damping factor or friction coefficient) of phonons in a phase transition mechanism is an adjusting phenomenological parameter for fitting between theory and experimental data. Yamada *et al.* have reported an Ising pseudospin – phonon coupled model for ammonium halides, in particular, for NH_4Br (Yamada *et al.* 1972). This model has been extended by Matsushita (Matsushita 1976). He considered the interactions between more than one pseudospin and one phonon. Matsushita derived the Hamiltonian for this model and by using perturbation theory he obtained the frequency and the damping constant of the phonons. According to Matsushita, the damping constant of a phonon is given by the imaginary part of its self energy (Matsushita 1976). The expressions that have been found for the damping constant are quite complicated and can hardly be used quantitavily without simplification. The expressions and the simplifications for the damping constant will be covered in the next chapter. Laulicht and Luknar have used Matsushita's theory to explain the damping constant in KH_2PO_4 (KDP) type crystals (Laulicht and Luknar 1977). According to them, the protons jump along the O-H bond from one XO_4^{3-} (X= P, As) ion to the other. This protonic motion is supposed to generate pseudospin waves (Blinc *et al.* 1974) which interact with all the phonons in the crystal and shorten their life time.

Activation energy can be defined in several ways, for example it can be defined as the minimum energy that is required for a chemical reaction to take place (chemical definition) or the energy that is required for the diffusion of the atoms or molecules within a solid or a fluid to move from their equilibrium position. In a different point of view, the definition of the activation energy can be explained in the following way: The activation energy is the energy which is required to create a

transition state (Hill and Dissado 1982). In the order-disorder ferroelectrics [$NaNO_2$, $(NH_4)_2SO_4$, etc.] each site can be considered to have a particle moving on a double minima potential surface. This energy is related to the damping constant and changes with the temperature, as we will see later.

1.2 Sodium Nitrite

Sodium nitrite, $NaNO_2$, which is a ferroelectric material undergoes an order-disorder phase transition at about 163 ^oC (Lamas *et al.* 1981)**.** Below this temperature, the structure of the $NaNO_2$ is orthorhombic and is polar along the b-axis with the space group C_{2v}^{2s} - Immm (Kay, Frazer 1961) and it is in the ferroelectric phase. In the narrow temperature range between the Neel temperature (T_N = 165.3 ^oC) and the Curie temperature (T_C = 163.9 ^oC), $NaNO_2$ is in sinusodial antiferroelectric phase(Yurtseven and Çaglar 2001). Above the Neel temperature, the structure of $NaNO_2$ is still orthorhombic but non- polar with space group D_{2h}^{25} - Immm (Komatsu *et al.* 1988) and it is in the disorder paraelectric phase. Phase transition from the disorder paraelectric phase into the ordered antiferroelectric phase, as the temperature decreases at Neel temperature, is a second order transition type (Tanisaki 1961) and phase transition from antiferroelectric phase to the ferroelectric phase as the temperature decreases further down the Curie temperature, is a first order phase transition type (Tanisaki 1961, 1963). The ferroelectric behaviour of sodium nitrite has been discovered by Sawada *et al*. (Sawada *et al*. 1958). After the discovery of this mechanism of phase transition, a lot of experimental and theoretical works have been carried out on $NaNO_2$. Calculation of the Brillouin frequencies close to phase transitions in $NaNO_2$ was studied by Yurtseven and

Çaglar (Yurtseven and Çaglar 2001). X- ray studies on $NaNO_2$ have been studied by Tanisaki (Tanisaki 1961, 1963) , Yamada *et al*. (Yamada *et al*. 1963), Hoshino and Motegi (Hoshino and Motegi 1967), and Durand *et al.* (Durand *et al.* 1982). There have been dielectric studies on $NaNO_2$ due to Sawada *et al.* (Sawada *et al. 1958*), Takagi and Gesi (Tagaki and Gesi 1964), Hamano (Hamano 1964) and Wyncke *et al*. (Wyncke *et al*. 1984). In addition to these experimental techniquies, calorimetric measurements for $NaNO_2$ have been done by Hoshino (Hoshino 1964) and Sakiyama *et al* (Sakiyama *et al 1965*). The thermal expansion and the elastic compliances of $NaNO_2$ have been performed by Ema *et al.* (Ema *et al. 1975*), and Hamano and Ema (Hamano and Ema 1978). There have been spectroscopic studies on $NaNO_2$. Vogt and Happ obtained far infrared absorption of $NaNO_2$ (Vogt and Happ 1968). Brehat and Wyncke have studied infrared spectra (Brehat and Wyncke 1985) and also Fahim has done a detailed infrared study on $NaNO_2$ (Fahim 2000). The reflection spectra have been studied by Axe (Axe 1968), and Barnoski and Ballantyne (Barnoski and Ballantyne 1968). Raman spectra for the $NaNO_2$ system have been reported in literature by Chisler and Shur (Chisler and Shur 1966, 1967) , Takase and Miyakawa (Takase and Miyakawa 1985), and Asawa and Barnoski (Asawa and Barnoski 1970). The ultrasonic and Brillouin scattering of $NaNO_2$ have been studied by Hatta *et al*. (Hatta *et al*. 1978, 1980), Shimizu *et al*. (Shimizu *et al*. 1974), Yagi *et al*. (Yagi *et al 1981, 1982*), Esayan *et al*. (Esayan *et al*. 1981), and Hatta (Hatta 1984). Buchheit *et al.* have used the spectroscopic technique, NMR, (Nuclear Magnetic Resonance) to investigate Na nucleus for the commensurate and incommunsurate phases in $NaNO_2$ (Buchheit *et al.* 1981). Sakurai *et al.* (Sakurai *et al. 1970*) and Durand *et al*. (Durand *et al 1986*.) have used the neutron spectroscopic technique to obtain the spectroscopic data for $NaNO_2$.

In addition to these experimental researches, some theoretical studies have been done on $NaNO_2$ to support these experimental studies. Tanisaki (Tanisaki 1961), Yamada *et al*. (Yamada *et al*. 1963), and Yamada and Yamada (Yamada and Yamada 1966) have applied an Ising model to the $NaNO_2$ system by using the analogy between the two possible orientations of an Ising spin (spin up and spin down) and the two equilibrium positions of the NO_2^- dipole in the paraelectric phase of $NaNO_2$. Erhardt and Michel (Erhardt and Michel 1981, 1981), and Fivez and Michel (Fivez and Michel 1983) have developed a microscopic model in their studies. By using the model propesed by Ishibashi and Shiba (Ishibashi and Shiba 1978), and Ishibashi *et al*. (Ishibashi *et al*. 1981) the mechanism of the phase transition in $NaNO_2$ has been explained. Klein *et al*. (Klein *et al*. 1982), and Lynden-Bell *et al*. (Lynden-Bell *et al*. 1984, 1986) have studied the critical fluctiations in the paraelectric phase of $NaNO_2$ by means of the molecular dynamics calculation. Naudts, in the meantime, has reported the incommensurate transition in $NaNO_2$ by using the mean field thory (Naudts 1983). Lamas *et al*. (Lamas *et al*. 1981) experimentally measured the order parameter using X-ray powder diffroctometry. Yurtseven *et al*. (Yurtseven *et al*. 2000) have studied the spontenous polarization close to phase transition in $NaNO_2$. Beccucci and Castellucci have studied the structural properties of $NaNO_2$ over a wide temperature range (Beccucci and Castellucci 1989). The structural change in $NaNO_2$ has been studied by Kay *et al.* (Kay *et al. 1975*) and by Ramondo (Ramondo 1989). The electronic structure of ferroelectric $NaNO_2$ was calculated by Ravindran *et al*. (Ravindran *et al*. 1999) and by Wang *et al*. (Wang *et al*. 2000). Phase diagram of $NaNO_2 + NaNO_3$ has been studied by Berg *et al*. (Berg *et al*. 2006).

1.3 Ammonium sulphate

Ammonium sulphate , $(NH_4)_2SO_4$, (hereafter AS), is a compound that has a first order phase transition from paraelectric phase to the ferroelectric phase at -49 ^{0}C (Mathias and Remeika 1956), without passing through an incommensurate phase or changing the size of the unit cell (Cummins 1990). AS has an orthorhombic Pnam-D_{2h}^{16} space group in the paraelectric phase (Wyckoff 1951, Rush and Taylor 1965, Dahlborg *et al.*1970) and an orthorhombic $Pna2_1$-C_{2v} space group in the ferroelectric phase (Schlemper and Hamilton 1966). There are four formula units (Z =4) per unit cell in both paraelectric and ferroelctric phases. The lattice constants of the paraelectric phase have been found as a=7.782 Å, b=10.636 Å, c=5.99 Å and for the ferroelectric phase a=7.837 Å, b=10.61 Å and c=5.967 Å (Rush and Taylor 1965). There are three reflection planes, namely, ab, bc, ca and a center of inversion for the paraelectric phase of AS at room temperature (Enginer *et al*. 2002). Because of the crystal symmetry in paraelectric phase of AS, a net dipole moment does not occur along any axis. In addition, the SO_4^{-2} ions and the two crystallographically inequivalent sets of NH_4^+ ions lie on the ab mirror planes in the paraelectric phase of AS (Enginer *et al*. 2002). On the other hand, the crystal is polarized only along the c-axis in the ferroelectric phase of AS at low temperature and there is neither ab plane of reflection nor center of inversion (O'Reilly and Tsang 1967, Badr and Awad 1984). The crystal structure of the AS in both paraelectric and ferroelectric phase have been reported in the literature by Rush and Taylor (Rush and Taylor 1965), Schlemper and Hamilton (Schlemper and Hamilton 1966), Hoshino *et al.*(Hoshino *et al*. 1958), Chiba (Chiba 1962), Torrie *et al*. (Torrie *et al*. 1972), Hasebe and Tanisaki

(Hasebe and Tanisaki 1977), and Hasebe (Hasebe 1981, 1981). The dielectric properties of AS have been reported by Matthias and Remeika (Matthias and Remeika 1956). Ikeda *et al*. (Ikeda *et al*. 1973) and Sawada *et* al. (Sawada *et* al. 1975) have studied the dielectric measurments of AS. Infrared spectroscopy of AS has been reported by Schutte and Heyns (Schutte and Heyns 1970) and by Jain *et al*.(Jain *et al*. 1973). Blinc *et al*. have studied the proton-nitrogen double resonance in AS (Blinc *et al*. 1972), and Nordland *et al*. have reported the dipolar relaxation time (T_{1D}) (Nordland *et al*. 1976). Raman measurement study has been performed by Torrie *et al* (Torrie *et al*. 1972) . NMR measurement studies have been done by O' Reilly and Tsang (O' Reilly and Tsang 1967), Blinc and Levstek (Blinc and Levstek 1960), Richards and Schaefer (Richards and Schaefer 1961), Watton *et al*. (Watton *et al*. 1972) and by Ramanathan and Srinivasan (Ramanathan and Srinivasan 1978). Neutron diffraction measurements have been reported by Rush and Taylor (Rush, J. J., and Taylor, T. I. 1965. Inelastic Scattering of Neutrons in Solids and Liquids. Proc. Bombay Symp., International Atomic Energy Agency, Vienna. P. 333.) and by Schlemper and Hamilton (Schlemper and Hamilton 1966). ESR (Electron Spin Resonance) studies have been done by Abe and Shibata (Abe and Shibata 1977), and by Fujimoto *et al*.(Fujimoto *et al*. 1977). Hoshino *et al*. have performed the thermal measurements of AS (Hoshino *et al*. 1958).

The mechanism of phase transitions in AS has also been supported by various theoretical models. The O'Reilly and Tsang's modified mean feld theory (O'Reilly and Tsang 1967) and Sawada's soft mode theory (Sawada et al. 1975) have been given. These two theories are based on the order- disorder type transition but Schlemper and Hamilton (Schlemper and Hamilton 1966) explained transitions in

terms of the changes in the H- bonding of the ammonium ion to the sulphate ion. They have stated that the transition is not an order-disorder type. In the O' Reilly and Tsang model (O' Reilly and Tsang 1967), the NH_4^+ tetrahedra are disorder with respect to the crystal ab plane and the reorientation of their dipoles of the disorder NH_4^+ tetrahedra is thought for the phase transition in AS. Unruh has observed the unique temperature dependence of the spontenous polarization (Unruh 1951, Unruh and Ayere) and this observation can be described by the model of Sawada *et al*. (Sawada *et al*. 1975) which is a two-sublattice model. Unruh has observed that the spontenous polarization increases suddenly to 6.0 10^{-7} $C.cm^{-2}$ and then decreases gradually at lower temperatures (Fujimoto *et al.* 1977). Unruh has named the polar phase below T_c as the ferrielectric phase (Unruh 1951) because of this unusual behaviour of the spontenous polarization. According to the ferrielectric model of Sawada *et al*. (Sawada *et al*. 1975), this ferrielectric phase has two oppositely polarized sublattices with two independent NH_4^+ ions in ammonioum halide unit cell. Phase transitions in AS have been explained in terms of an Ising model by Hasebe (Hasebe 1981). He has defined two Ising variables to specify the orientations of the two independent NH_4^+ ions since each ammonioum ion distorts, carries a permenant dipole in both below T_c (ferroelectric phase) and above T_c (paraelectric phase). Hasebe has defined these two Ising variables by considering the coupling between the pseudospins and the phonon in AS. Unruh (Unruh 1965), Onodera *et al*. (Onodera *et al*. 1978, 1985), and Syamaprasad and Vallabhan (Syamaprasad and Vallabhan 1981) have reported the dielectric constant studies in the literature. The temperature dependence of the spontenous polarization directly effects the dielectric

constant near the paraelectric-ferrielectric phase transition in AS. According to the studies reported in the literature (O' Reilly and Tsang 1967, Onodera *et al*. 1978), the dielectric anomally in AS is quite small, and the temperature dependence is very weak. Unruh has stated that the relative dielectric constant follows Curie-Weiss law in the paraeleytric phase (Unruh 1965). Onodera *et al*. (Onodera *et al*. 1978, 1985) have modeled the dielectric constant to investigate the mechanism of phase transition in AS. They have reported two models. In the first model, Onodera *et al.* have expanded the Gibbs free energy in terms of the two polarizations P_1 and P_2, with a linear coupling P_1 P_2 (Onodera *et al*. 1978). In the second model, they have expanded the Gibbs free energy in terms of the polarization P_1 and P_2 up to the $P_1^4(P_2^4)$ terms with the linear coupling P_1 P_2 (Onodera *et al*. 1985). They have considered the dipole-dipole interaction in AS, and by using this consideration they have obtained the critical behaviour of the spontaneous polarization and the dielectric susceptibility. The temperature dependence of the susceptibility has been studied by Enginer *et al*. (Enginer *et al*. 2002) by expanding the Gibbs free energy in terms of the polarization P_1 and P_2 up to the $P_1^4(P_2^4)$ in a two sublattice model with the quadratic coupling term P_1^2 P_2^2. In their study, Enginer *et al*. have considered the quadrupole-quadrupole interactions in AS. Grecu *et al*. (Grecu *et al*. 2003) have reported the results of EPR (Electron Paramagnetic Resonance) and Mössbauer investigations on lattice dynamics in AS experimentally. Optical studies of the AS single crystal in the paraelectric phase have been reported by El-Korashy *et al.* (El-Korashy *et al. 2003*). Raman scattering study of ferroelectric phase transition in AS has been reported by Iqbal and Christoe (Iqbal and Christoe 1976).

THEORY

2.1 Classification of the Phase Transitions

A phase transition occurs when a phase that is described with intensive variables such as pressure (P), temperature (T), magnetic field ($\vec{H}$), electric field ($\vec{E}$) , etc, becomes unstable (discontinuous) in the given thermodynamic conditions. In other words, if there is a singularity in the free energy of the one of its derivatives, then a phase transition occurs. Ehrenfest has divided the phase transitions thermodynamically into two classes.

First order transitions: In this type of phase transitions, there is discontuinity in the quantities such as entropy (S), and volume (V) which are the first derivatives of the relevant thermodynamic potentials. First order transitions are the transitions with latent heat. The entropy and the volume are given by

$$S = -(\frac{\partial G}{\partial T})_{\mathrm{P}} \quad \text{and} \quad V = (\frac{\partial G}{\partial P})_{\mathrm{T}} \tag{2.1}$$

where G(P,T) is the Gibbs free energy and described by the variables P and T.

Second order transitions: In this type of transition the thermodynamic potential and its first derivatives are continuous but some quantities such as specific heat at constant pressure, C_P, and compressibility at constant temperature, κ_T, which are the second derivatives of the potential with respect to temperature and pressure, respectively, approach infinity at the transition point These quantities are given as following

$$C_P = -T(\frac{\partial^2 G}{\partial T^2})_P = T(\frac{\partial S}{\partial T})_P \quad \text{and} \quad \kappa_T = -\frac{1}{V}(\frac{\partial^2 G}{\partial P^2})_T = -\frac{1}{V}(\frac{\partial V}{\partial P})_T \qquad (2.2)$$

2.2 Order Parameter

Order parameter measures the orderness in a sample. In this part of the study, we will derive an expression for the order parameter and also investigate this expression in a temperature range from low temperatures to the above the transition temperature T_c. Bragg and Williams described a transition observed in brass (alloy of the copper (Cu) and zinc (Zn)) in 1934.They brought up that, the groups of the brass atoms are ordered in a crystal lattice (Papon *et al.* 2001).This phenomenon has been proven by using X-ray spectra. X-ray measurements showed that all of the Zn atoms are ordered in one lattice and all of the Cu atoms are ordered in another lattice, where these lattices are interpenetrated. Cubic symmetry exists in this ordered lattice. A specific heat peak that is characteristic of a second order transition at the critical temperature is observed. These observations have been used as a standart to study phase transitions in ferromagnetics, supercunductors, liquid crystals, etc.

Here we assume that there are two different atoms, A and B equally positioned in two types of sites α and β. Each α site is surrounded by β sites and

each β site is surrounded by α sites. Here α and β sites are the nearest neighbours. At very low temperatures, the system is completely ordered. This means that at very low temperatures the interaction energy between two different neighbouring atoms, which is given by V_{AB}, is lower than the avarage interaction energy between atoms of the same species, $\frac{V_{AA}+V_{BB}}{2}$. Here all A atoms occupy α sites and all B atoms occupy β, this is the lowest energy arrangement for the system.

The order parameter, P, has been defined as follows,

$$P = \frac{p_\alpha - 1/2}{1/2} \tag{2.3}$$

where p_α is the probability that an α site will be occupied by an A atom. By using this definition, number of pairs, that is N_{AA}, N_{BB}, N_{AB} has been calculated as,

$$N_{AA} = N_{BB} = N(1-P^2) \quad \text{and} \quad N_{AB} = 2N(1+P^2) \tag{2.4}$$

Here, N is the total number of sites ($\frac{N}{2}$ α sites and $\frac{N}{2}$ β sites). Then by assuming only the nearest neighbour interactions, the internal energy can be written as,

$$U = U_0 + NP^2V \tag{2.5}$$

where

$$U_0 = N(V_{AA}+V_{BB}+2V_{AB}) \quad \text{and} \quad V = 2V_{AB} - V_{AA} - V_{BB} \tag{2.6}$$

Then, the number of ways for the A and B atoms that can be distributed in the α and β sites or the number of configurations (W) is given by,

$$W = \frac{(N/2)!}{\left[\left(\frac{1+P}{4}\right)N\right]!\left[\left(\frac{1-P}{4}\right)N\right]!} \frac{(N/2)!}{\left[\left(\frac{1-P}{4}\right)N\right]!\left[\left(\frac{1+P}{4}\right)N\right]!} \tag{2.7}$$

By using Boltzman equation given by,

$$S = k \log W \tag{2.8}$$

the entropy (S) can be calculated by using Stirling's approximation. Here, k is the Boltzman constant. Then, the free energy, F , can be calculated by inserting (2. 5) and (2. 8) in the following equation given by

$$F = U - TS \tag{2.9}$$

So that the free energy is,

$$F = U_0 + VNP^2 - \left(\frac{kTN}{2}\right)\{2\log 2 - [(1+P)\log(1+P) + (1-P)\log(1-P)]\} - TNS_0 \tag{2.10}$$

Where S_0 is the entropy of the A and B atoms in their lattice. F should be minimum at thermodynamic equilibrium. In other words, the first derivative of the free energy with respect to order parameter should be zero. So,

$$\frac{\partial F}{\partial P} = 2NPV + \frac{NkT}{2}\log\left(\frac{1+P}{1-P}\right) = 0 \tag{2.11}$$

The roots of this equation can be found graphically or by some approximation (Taylor expansion of the logarithmic term) and by the definition of the critical temperature given by,

$$kT_C = -2V \tag{2.12}$$

one can show that;

$$P \approx \pm\sqrt{3\frac{T_C - T}{T}} \qquad \text{for} \quad T\langle T_C \ \text{ and } \ P = 0 \ \text{ if } \quad T\rangle T_C \tag{2.13}$$

This calculation holds only if $P\langle\langle 1$. The order parameter has an infinite slope at T_C .

From (2.11) , in the case of $T \langle\langle T_C$ we can write,

$$P \approx \tanh\left(\frac{-PT_C}{T}\right) \tag{2.14}$$

So that, at very low temperature,

$$P \approx 1 - 2\exp\left(\frac{-2T_C}{T}\right) \tag{2.15}$$

To sum up, the order parameter, in general, is given by,

$$P \approx \begin{cases} 1 - 2\exp\left(\dfrac{-2T_C}{T}\right) & T \langle\langle T_C \\ \left\{3\left(1 - \dfrac{T}{T_C}\right)\right\}^{\frac{1}{2}} & 0 \langle (T_C - T) \langle T_C \\ 0 & T_C \langle T \end{cases} \tag{2.16}$$

2.3 Damping Constant

In this study we use the Ising spin-phonon coupled system introduced initially by Yamada et al. (Yamada *et al.* 1972) and later by Matsushita (Matsushita 1976) to explain the phase transitions both in $NaNO_2$ and $(NH_4)_2SO_4$. It has been reported that in the paraelectric phase of $NaNO_2$ (above T_C), the nitrogen atom of the NO_2^- ion appears to randomly jump to either the left or the right crystallographic plane (Shibuya 1961 and Gesi 1965). On the other hand, there is an ordered undirectional alignment of the NO_2^- dipole that is related to the displacement of the Na^+ ions along the b-axis (Hartwig *et al.* 1971).

O' Reilly and Tsang (O' Reilly and Tsang 1967) considered an order-disorder process involving the distorted NH_4^+ ions in the lattice for $(NH_4)_2SO_4$. At

low temperatures (ferroelectric phase) of the $(NH_4)_2SO_4$, the NH_4^+ ions are oriented parallel to each other while at high temperatures (paraelectric phase) all the NH_4^+ tetrahedra are randomly distrubuted (up or down orientations).

It is considered for the $NaNO_2$ and $(NH_4)_2SO_4$ that the orientations of the NO_2^- dipole and NH_4^+ tetrahedra are eigenstates of Ising spins and also it is considered that the nearest neighbour interactions between spins are the exchange interactions.

Yamada *et al*.(Yamada *et al.* 1972) reported an Ising pseodospin-phonon coupled model by only considering one pseodospin and one phonon. Matsushita (Matsushita 1976) has extended this model by assuming more than one pseodospin and more than one phonon. His Hamiltonian is given as (Matsushita 1976),

$$H = \frac{1}{2}\sum_{\vec{k}\upsilon}\left[P^*(\vec{k}\upsilon)P(\vec{k}\upsilon) + \omega_0^2(\vec{k}\upsilon)Q^*(\vec{k}\upsilon)Q(\vec{k}\upsilon)\right] - \frac{1}{2}\sum_{\vec{q}} J_{eff}(\vec{q})\sigma^*(\vec{q})\sigma(\vec{q})$$

$$+ \sum_{\vec{k}\,\vec{q}\,\upsilon\upsilon'} K_{1,eff}(\vec{k}\,\vec{q}\,\upsilon\upsilon')\sigma(\vec{q})Q^*(\vec{k}\upsilon)Q(\vec{k}-\vec{q},\upsilon')$$

$$+ \sum_{\vec{k}\,\vec{q}\,\vec{q}'\,\upsilon\upsilon'} K_{2,eff}(\vec{k}\,\vec{q}\,\vec{q}'\,\upsilon\upsilon')\sigma(\vec{q})\sigma(\vec{q}')Q^*(\vec{k}\upsilon)\times Q(\vec{k}-\vec{q}-\vec{q}',\upsilon') + H_A \tag{2.17}$$

where

$$J_{eff}(\vec{q}) = J(\vec{q}) + \sum_{\upsilon}\left|g(\vec{q}\,\upsilon)\right|^2 \tag{2.18}$$

In this Hamiltonian, the first two terms define the phonon energy, P is the momentum of the phonon with the wave vector $\vec{k}$ and mode υ, Q is its coordinate

in the canonical form (Kanomori *et al*. 1968) and, ω_0 is the characteristic frequency of the corresponding phonon. J_{eff}, appearing in the second term, is the interaction energy between the two pseudospins. The coefficient $K_{1,eff}$ represents the interaction between one pseudospin and two phonons, while the coefficient $K_{2,eff}$ correspond to the interaction between two pseudospin and two phonons. Both of these two coefficients are related to the lattice and force constants. These coefficients are used to define the reorientation of the NH_4^+ ions (Matsushita 1976) and, g is the copling constant that couples a pseudospin to a phonon. Matsushita has derived the damping constant , Γ_{SP} , for the pseudospin-phonon coupling by using his Hamiltonian. It is given as,

$$\Gamma_{SP}(\vec{k}\upsilon,\omega) = \sum_{\vec{q}\,\upsilon'} \frac{\left|K_1(\vec{k},\vec{q},\upsilon,\upsilon')\right|^2}{8\omega\omega_0(\vec{k}-q,\vec{\upsilon}')}$$

$$\times\{[\frac{\mathrm{n}(\omega_0(\vec{\mathrm{k}}\text{-}\vec{\mathrm{q}},\upsilon'))}{\mathrm{n}(\omega\text{-}\omega_0(\vec{\mathrm{k}}\text{-}\vec{\mathrm{q}},\upsilon'))+1}+1]\times \mathrm{S}(\vec{\mathrm{q}},\omega\text{-}\omega_0(\vec{\mathrm{k}}\text{-}\vec{\mathrm{q}},\upsilon'))$$

$$+[\frac{\mathrm{n}(\omega_0(\vec{\mathrm{k}}\text{-}\vec{\mathrm{q}},\upsilon'))+1}{\mathrm{n}(\omega+\omega_0(\vec{\mathrm{k}}\text{-}\vec{\mathrm{q}},\upsilon'))+1}+1]\times \mathrm{S}(\vec{\mathrm{q}},\omega+\omega_0(\vec{\mathrm{k}}\text{-}\vec{\mathrm{q}},\upsilon'))\}$$

(2.19)

$S(\vec{q},\omega)$ is known as the scattering function of the pseudospins. Laulicht and Luknar (Laulicht and Luknar 1972) used the following approximation in order to simplify the Eq.2.19.

1- $\Gamma(\vec{k}\upsilon,\omega) \cong \Gamma(\vec{k}\upsilon,\omega_\upsilon)$, where ω_υ is the peak frequency with a Lorentzian line shape. $\omega_\upsilon = \omega_0(\vec{k},\upsilon) \approx \omega_0(\vec{k}-\vec{q},\upsilon)$.

2- Near the critical temperature (T_C), K_1, $\omega_0(\vec{k}-\vec{q},\upsilon)$ and n are weakly dependent on q and T.

3- An integral replaced over all q in the Brillouin zone instead of the summation in Eq. 2.19.

The dynamic scattering function of the pseudospins, $S(\vec{q},\omega)$, is a Debye type below T_C and its value is strongly dependent on temperature at low frequencies near T_C (Blinc and Zeks, Soft Modes in Ferroelectrics and Antiferroelectrics, 1976). The dominant term corresponds to the replacing $\upsilon' = \upsilon$ in Eq.(2.19) (Laulicht 1978). So, $S(\vec{q},\omega_\upsilon(\vec{k}) - \omega_0(\vec{k}-\vec{q})) \cong S(\vec{q},\omega \approx 0)$. All the terms multiplied by $S(\vec{q},\omega \rangle\rangle 0)$ are weakly temperature dependent since they correspond to the very far wing of a line with a peak at $\omega = 0$.

By doing these approximations, Laulicht and Luknar obtained the following temperature dependent damping constant expression (Laulicht and Luknar 1976).

$$\Gamma(\vec{k}\upsilon,\omega_\upsilon) = \Gamma_0 + A(1-P^2)\ln\left(\frac{T_C}{T - T_C(1-P^2)}\right) \qquad (2.20)$$

where Γ_0 is the background damping constant and it is independent of temperature , A is a constant and P is the order parameter.

Schaak and Winterfeldt also obtained a similar expression to the Eq.(2.20) for the temperature dependence of the damping constant due to the pseudospin-phonon interaction (Schaak and Winterfeldt 1977). This is given by,

$$\Gamma_{SP}(\omega_{\upsilon}) = \Gamma_0' + A'[\frac{T(1 - P^2)}{T - T_C(1 - P^2)}]^{\frac{1}{2}} \tag{2.21}$$

where Γ_0' is the background damping constant and it is independent of temperature, and A' is a constant.

2.4 Activation Energy

Activation energy is the energy barrier separating the different orientation of the ion groups in the phase transitions (Fahim 2000). These ion groups are the NO_2^- ions in $NaNO_2$ and NH_4^+ ions in $(NH_4)_2SO_4$. Both in $NaNO_2$ and $(NH_4)_2SO_4$, the phase transitions are related to the reorientational motion of the NO_2^- ions and NH_4^+ ion**s.** Bartoli and Litovitz (Bartoli and Litovitz 1972) and Rakov (Rakov 1959) have reported the total linewidth as a function of temperature as follows,

$$\Gamma \cong \Gamma_{vib} + C\exp(\frac{-U}{k_B T}) \tag{2.22}$$

where U is the activation energy, k_B is the Boltzman constant, and C is a constant. The first term in Eq. (2.22) corresponds to the vibrational relaxation process and the second term is related to the reorientational relaxation process. Sathaiah and Bist suggested that to get information about the reorintational relaxation process, the vibrational relaxtaion can be ignored or treated as temperature independent over the short range of temperature close to the critical temperature (Sathaiah and Bist 1991). By doing this approximation, they revised the Eq.(2.22) for the Lithium Ammonium

Sulphate (LAS) like crystals. In a LAS type crystal, the ferroelectric transition is governed by the reorientational relaxation process (Abul Hossain *et al.* 1993). After this approximation, the relation between damping constant and the activation energy at various temperatures is given by

$$\ln \Gamma = -(\frac{U}{k_B T}) \tag{2.23}$$

Where U is the activation energy of the reorientatinal motion of the sulphate ion.

In this study, the activation energy of the modes that appear both in $NaNO_2$ and $(NH_4)_2SO_4$ has been calculated according to Eq.(2.23).

CALCULATIONS

3.1 Calculation of the Order Parameter, Damping Constant and the Activation Energy as a function of Temperature close to the Phase Transition Point for the Raman mode of B_1 asymmetric in $NaNO_2$.

Matsushita, as we covered in the Theory subsection 2.2, has given an expression for the order parameter as a function of temperature by using the molecular field theory and considering the reorientational motion of the NH_4^+ in ammonium halides (Matsushita, 1967). In this part of the study, we consider the reorientational motion of the NO_2^- ions and calculate the order parameter using two expressions separately according to Eq. (2.16). The temperature range for $NaNO_2$ is from 400 K to 434 K (Hartwig *et al.* 1971) and the critical temperature is 436 K (Lamas *et al.* 1981). We extrapolated the temperature range from 400 K to 280 K. We plotted the order parameter versus temperature graph in Fig. 3.1.1 and order parameter squared versus temperature graph in Fig.3.1.2.

By fitting the Eq. 2.20 to the observed Raman bandwiths for the B_1 asymmetric mode of $NaNO_2$, we calculated the background constant, Γ_0, and constant A. Our results are $\Gamma_0 = 7.8353$ cm^{-1} and $A = 7.7761$ cm^{-1}. Likewise, we fitted Eq. 2.21 to the bandwiths of this mode and calculated Γ_0' and A' as 14.7508 cm^{-1} 3.0872 cm^{-1}, respectively. Those values are given in Table 3.1.1. The observed Raman bandwidths (Hartwig *et al.* 1971) and the damping constant, Γ, calculated by means of Eq.

(2.20) and Eq. (2.21) as a function of temperature for the B_1 asymmetric Raman mode of the $NaNO_2$ are plotted in Fig. 3.1.3.

The activation energy of the B_1 asymmetric Raman mode of the $NaNO_2$ has been calculated by using Eq. (2.23). Here, we plot the $\ln\Gamma$ versus $\frac{1}{T}$ graphs (Arrhenius plot) for each damping constant calculated from Eq. (2.20) and Eq. (2.21). In Fig. 3.1.4 and Fig. 3.1.5, we used the damping constant calculated from Eq. (2.20) while we used the damping constant calculated from Eq. (2.21) in Fig. 3.1.6 and Fig. 3.1.7. The temperature range for the Fig. 3.1.4 is from 433.8 K to 427 K and the activation energy, U, is calculated as 0.7512 eV. The temperature range in Fig.3.1.5 is from 424.3 K to 402.8 K and the activation energy is calculated as 0.2825 eV. In Fig. 3.1.6, the temperature range is from 433.8 K to 427 K and the activaton energy is 0.9852 eV. In Fig. 3.1.7 the temperature range is from 424.3 K to 402.8 K and the activation energy is 0.1705 eV. All these activation energy values are given in Table 3.1.2.

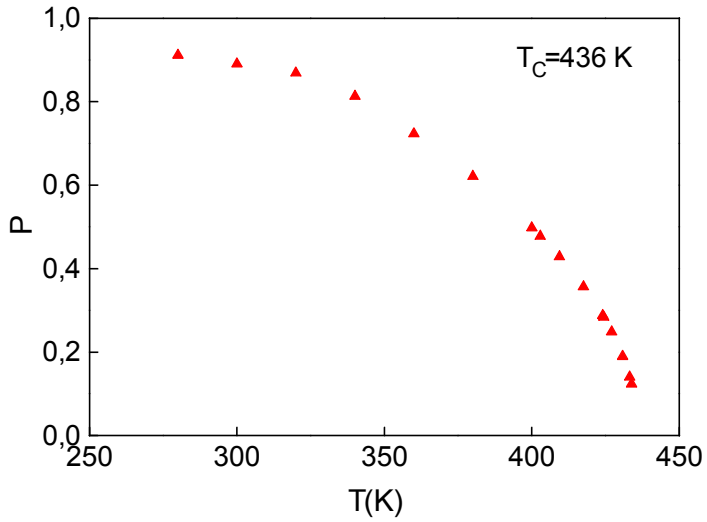

Figure 3.1.1 Order parameter, P, as a function of temperature for $NaNO_2$ according to Eq.(2.16) from the molecular field theory (T_C= 436 K).

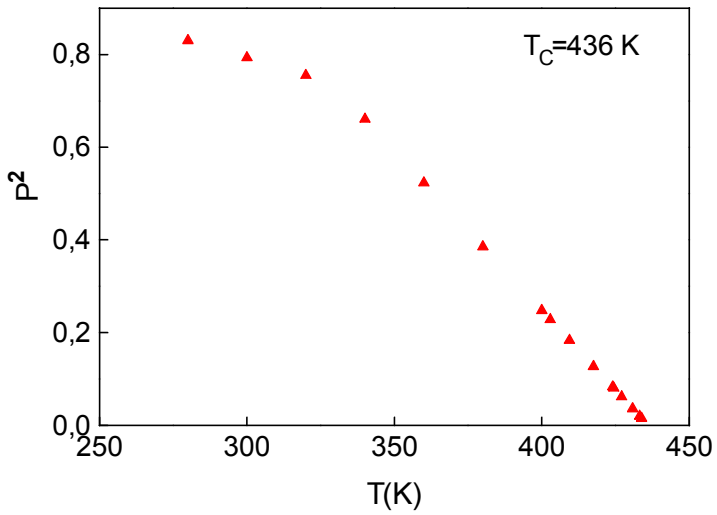

Figure 3.1.2 Order parameter squared,P^2, as a function of temperature for $NaNO_2$ according to Eq.(2.16) from the molecular field theory (T_C= 436 K).

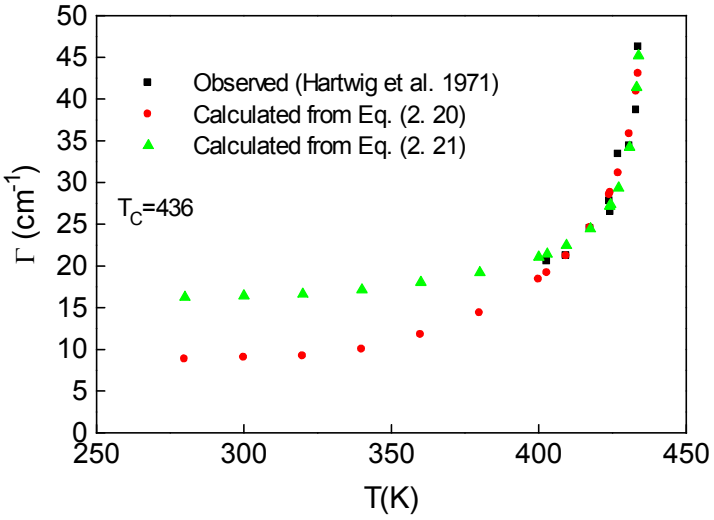

Figure 3.1.3 Damping constant calculated from Eqs. (2.20 and 2.21) as a function of temperature for the B_1 asymmetric Raman mode of $NaNO_2$ (T_C= 436 K). The observed bandwidths of this mode are also plotted here (Hartwig *et al.* 1971).

Table 3.1.1 Values of the background bandwidth Γ_0 and the coefficient A (Eq. 2.20), and values of Γ_0' and A' (Eq. 2.21), for the B_1 asymmetric Raman mode of $NaNO_2$ in the ferroelectric phase (436 K).

Crystal	Raman mode	$\Gamma_0(cm^{-1})$	$A(cm^{-1})$	$\Gamma_0'(cm^{-1})$	$A'(cm^{-1})$
$NaNO_2$	B_1 asymmetric	7.8353	7.7761	14.7508	3.0872

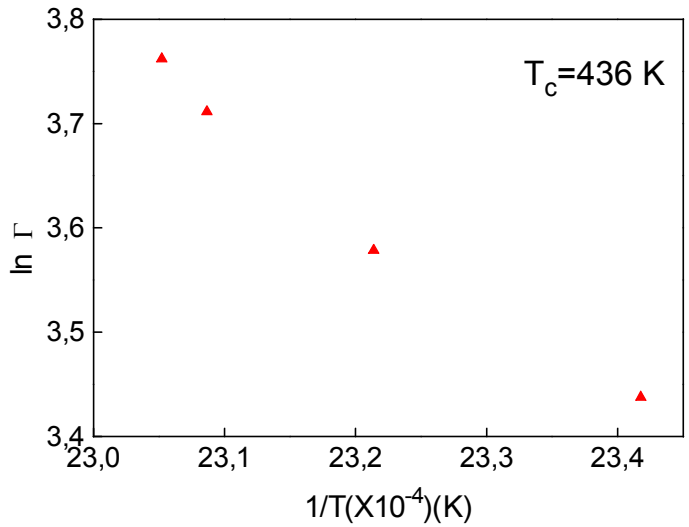

Figure 3.1.4 A plot of $\ln\Gamma$ vs $1/T$ (Arrhenius plot) for the B_1 asymmetric Raman mode of $NaNO_2$ for the temperature interval indicated to calculate the activation energy according to Eq. (2. 23). (The damping constants used here, have been calculated from Eq. (2. 20)).

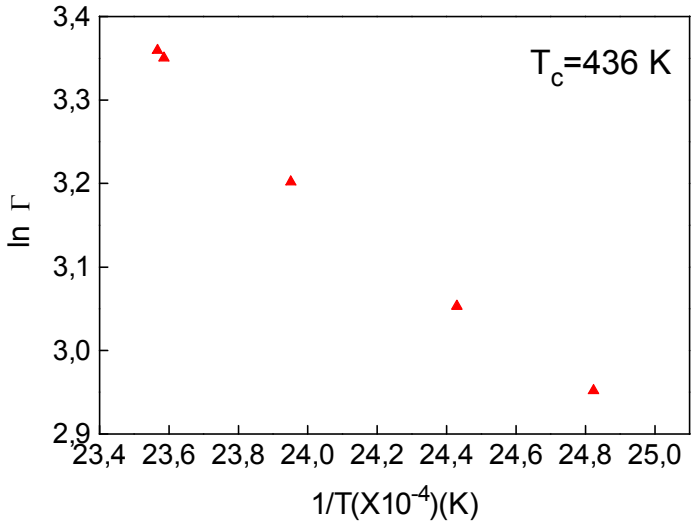

Figure 3.1.5 A plot of $\ln\Gamma$ vs $1/T$ (Arrhenius plot) for the B_1 asymmetric Raman mode of $NaNO_2$ for the temperature interval indicated to calculate the activation energy according to Eq. (2. 23). (The damping constants used here, have been calculated from Eq. (2. 20)).

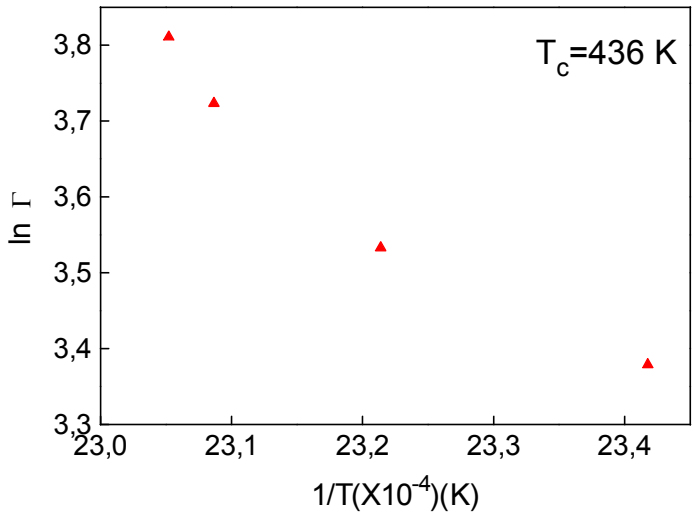

Figure 3.1.6 A plot of $\ln\Gamma$ vs $1/T$ (Arrhenius plot) for the B_1 asymmetric Raman mode of $NaNO_2$ for the temperature interval indicated to calculate the activation energy according to Eq. (2. 23). (The damping constants used here, have been calculated from Eq. (2. 21)).

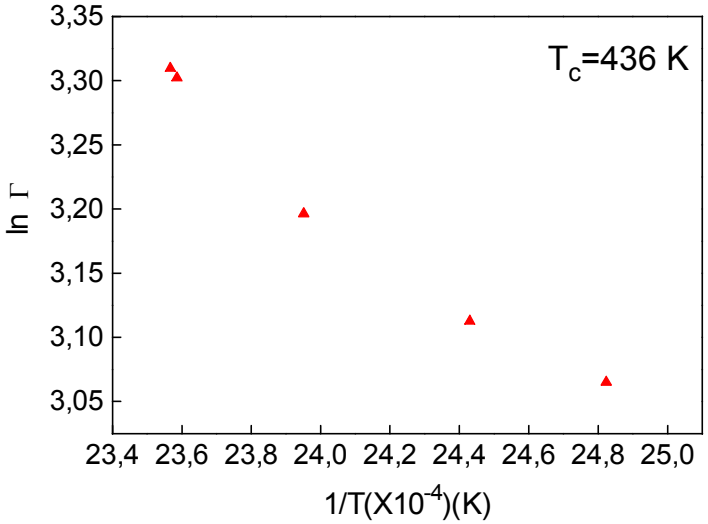

Figure 3.1.7 A plot of $\ln\Gamma$ vs $1/T$ (Arrhenius plot) for the B_1 asymmetric Raman mode of $NaNO_2$ for the temperature interval indicated to calculate the activation energy according to Eq. (2. 23). (The damping constants used here, have been calculated from Eq. (2. 21)).

Table 3.1.2 Values of the activation energy U calculated in the temperature interval for the B_1 asymmetric Raman mode of $NaNO_2$ according to Eq. (2. 23) where the damping constant (Eqs. 2.20 and 2. 21) was used in the ferroelectric phase (T_C= 436 K).

Crystal	Raman mode	Damping Constant	Temperature range T(K)	Activation energy (eV)	k_BT_C (eV)
$NaNO_2$	B_1 asymmetric	Eq. (2.20)	433.8 < T < 427	0.7512	0.0376
			424.3 < T < 402.8	0.2825	
		Eq. (2.21)	433.8 < T < 427	0.9852	
			424.3 < T < 402.8	0.1705	

3.2 Calculation of the Damping Constant and the Activation Energy as a function of Temperature close to the Phase Transition Point for the Raman mode of B_2 libration in $NaNO_2$.

The temperature range for $NaNO_2$ is from 400 K to 435.7 K (Hartwig *et al.* 1971) **.** We extrapolated the temperature from 400 K to 280 K. The critical temperature is 436 K (Lamas *et al.* 1981)**.**

We fitted Eq. (2.20) and Eq. (2.21) to the observed Raman bandwidths for the B_2 libration mode of $NaNO_2$. The background constants and the coefficients that appear in Eq. (2.20) and Eq. (2.21) have been found as Γ_0=40.2457 cm^{-1}, A=3.1153 cm^{-1}, Γ_0'=47.8767 cm^{-1} and A'=0.4479 cm^{-1}. Those values are given in Table 3.2.1. The oberved Raman bandwidths (Hartwig *et al*. 1971) and the damping constant calculated from Eq. (2.20) and Eq. (2.21) as a function of temperature for the B_2 libration mode in $NaNO_2$ are plotted in Fig. 3.2.3.

We computed here the activation energy of the B_2 libration Raman mode of $NaNO_2$ with help of the Eq. (2.23). We calculated the activation energy for two temperatures range. In Fig. 3.2.4, we plot $\ln\Gamma$ versus $\frac{1}{T}$ graph (Arrhenius plot). Here, the temperature range is from 435.7 K to 429.3 K and the activation energy is calculated as 0.4461 eV. Likewise, In Fig. 3.2.5 the temperature range is from 431.3 K to 421.3 K and the activation is found as 0.1251 eV. The damping constant, Γ, that appear in Fig. 3.2.4 and in Fig. 3.2.5 is calculated from Eq. 2.20. In Fig. 3.2.6, the temperature range varies between 435.7 K and 431.1 K and the activation energy is 0.6389 eV. The temperature range for Fig. 3.2.7 is from 431.4 K to 421.3 K and the activation energy is 0.0420 eV. The damping constant, Γ, in Fig. 3.2.6 and in Fig. 3.2.7 is calculated from Eq. (2.21). All these activation energy values are given in Table 3.2.2.

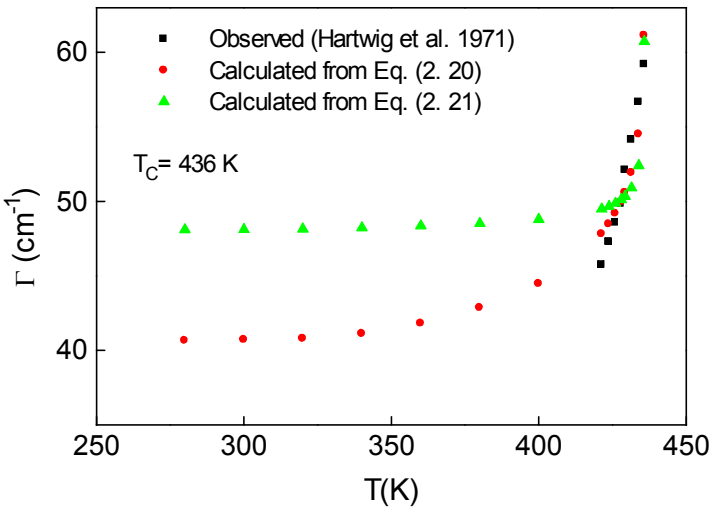

Figure 3.2.1 Damping constant calculated from Eqs. (2.20) and (2.21) as a function of temperature for the B_2 libration Raman mode of $NaNO_2$ (T_C= 436 K). The observed bandwidths of this mode are also plotted here (Hartwig *et al.* 1971).

Table 3.2.1 Values of the background bandwidth Γ_0 and the coefficient A (Eq. 2.20), and values of Γ_0' and A' (Eq. 2.21), for the B_2 libration Raman mode of $NaNO_2$ in the ferroelectric phase (436 K).

Crystal	Raman mode	$\Gamma_0(cm^{-1})$	$A(cm^{-1})$	$\Gamma_0'(cm^{-1})$	$A'(cm^{-1})$
$NaNO_2$	B_2 libration	40.2457	3.1153	47.8767	0.4479

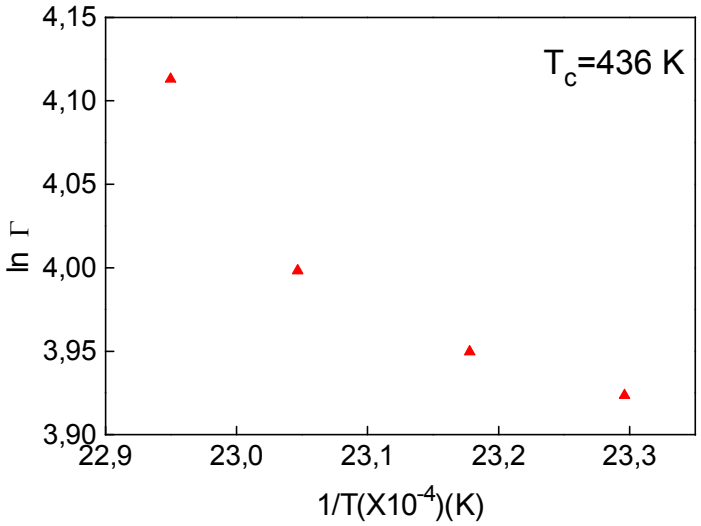

Figure 3.2.2 A plot of $\ln\Gamma$ vs $1/T$ (Arrhenius plot) for the B_2 libration Raman mode of $NaNO_2$ for the temperature interval indicated to calculate the activation energy according to Eq. (2. 23). The damping constants used here, have been calculated from Eq. (2. 20)).

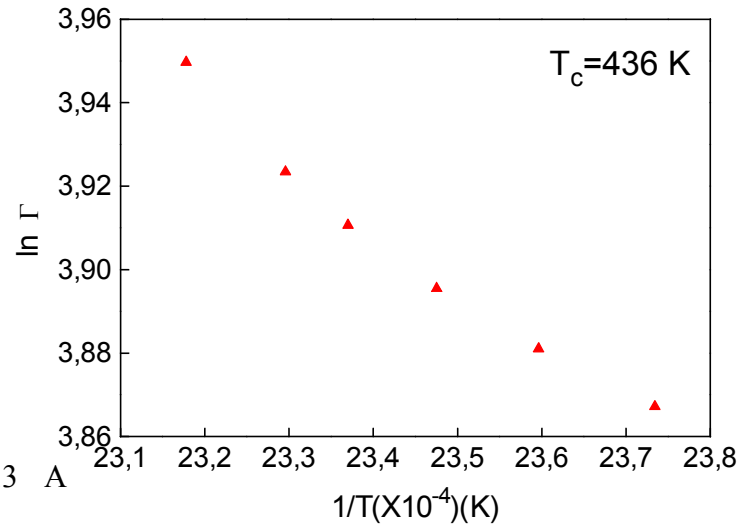

Figıre 3.2.3 A plot of $\ln\Gamma$ vs $1/T$ (Arrhenius plot) for the B_2 libration Raman mode of $NaNO_2$ for the temperature interval indicated to calculate the activation energy according to Eq. (2. 23). (The damping constants used here, have been calculated from Eq. (2. 20)).

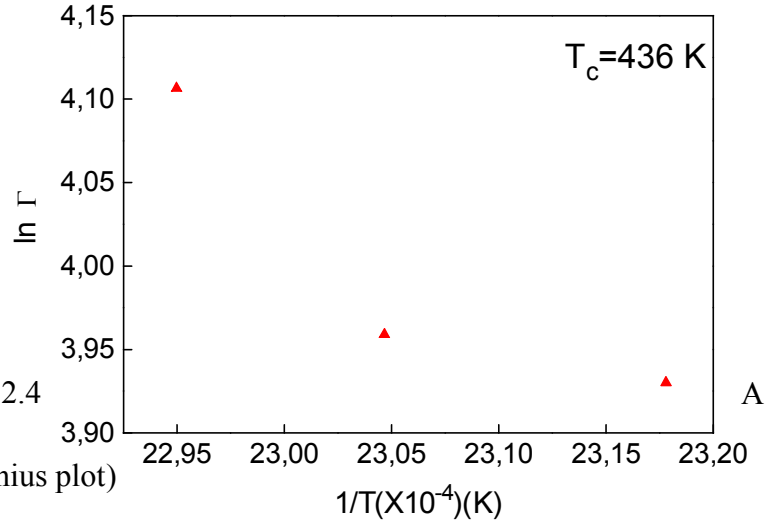

Figure 3.2.4 A plot of $\ln\Gamma$ vs $1/T$ (Arrhenius plot) for the B_2 libration Raman mode of $NaNO_2$ for the temperature interval indicated to calculate the activation energy according to Eq. (2. 23). (The damping constants used here, have been calculated from Eq. (2. 21)).

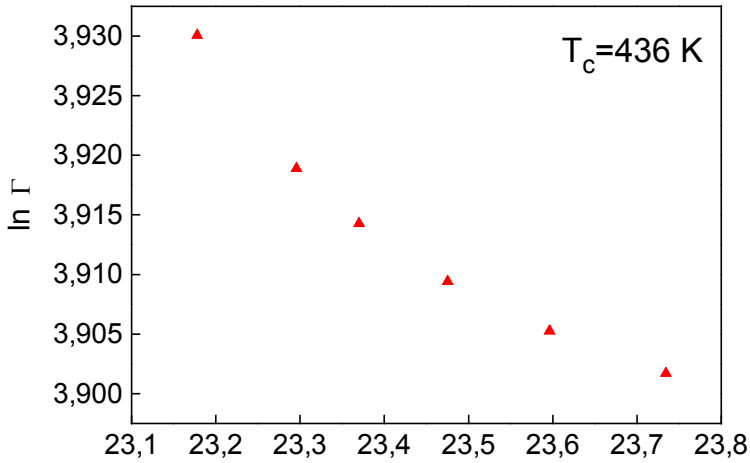

Figure 3.2.5 A plot of $\ln\Gamma$ vs $1/T$ (Arrhenius plot) for the B_2 libration Raman mode of $NaNO_2$ for the temperature interval indicated to calculate the activation energy according to Eq. (2. 23). (The damping constants used here have been calculated from Eq. (2. 21)).

Table 3.2.2 Values of the activation energy U calculated in the temperature interval for the B_2 libratinal Raman mode of $NaNO_2$ according to Eq. (2. 23) where the damping constant (Eqs. 2.20 and 2. 21) was used in the ferroelectric phase (T_C= 436 K).

Crystal	Raman mode	Damping Constant	Temperature range T(K)	Activation energy (eV)	k_BT_C (eV)
$NaNO_2$	B_2 libration	Eq. (2.20)	435.7 < T < 429.3	0.4461	0.0376
			431.3 < T < 421.3	0.1251	
		Eq. (2. 21)	435.7 < T < 431.1	0.6389	
			431.4 < T < 421.3	0.0420	

3.3 Calculation of the Damping Constant and the Activation Energy as a function of Temperature close to the Phase Transition Point for the Raman mode of B_1 libration in $NaNO_2$.

The values of the order parameter calculated from molecular field theory, Eq. (2.16), are used to evaluate the damping constant as a function of temperature. Eqs. 2.20 and 2.21 have been fitted to the observed Raman bandwidths for the B_1 librational Raman mode of $NaNO_2$. The background constant Γ_0 and coefficient A in Eq. (2.20) have been found as 13.0586 cm^{-1} and 3.4127 cm^{-1}, respectively. Likewise, Γ_0' and A' in Eq. (2.21) have been found as 19.6212 cm^{-1} and 0.6356 cm^{-1}, respectively. We tabulated these values in Table 3.3.1. Damping constants calculated from Eqs. (2.20) and (2.21) and the observed Raman bandwidths (Hartwig *et al*. 1971) as a function of temperature for the B_1 libration Raman mode in $NaNO_2$ have been plotted in Fig. 3.3.3.

Activation energy of this mode of $NaNO_2$ has been calculated by using Eq. (2.23). The activation energy in the temperature range of $435.6 < T(K) < 429.3$ has been found as 1.1480 eV while it is 0.1362 eV in the temperature range of $429.3 < T(K) < 411.8$. These activation energy values have been calculated with help of the slopes of the Fig. 3.3.4 and Fig. 3.3.5 respectively. Both of these two graphs are Arrhenius plots ($\ln\Gamma$ versus $\frac{1}{T}$). Damping constants used in these two graphs have been calculated from Eq. (2.20). Similarly, we used the damping constant values calculated from Eq. 2.21 to evaluate the activation energy values with help of the Arrhenius plots for the two temperature range given above. In Fig. 3.3.6, we calculated the activation energy as 0.9439 eV in temperature range of $435.6 < T(K) < 429.3$, and in Fig. 3.3.7, we calculated the activation energy as 0.0852 eV in

temperature range of 429.3 < T(K) < 411.8. We tabulated these avtivation energy values in Table 3.3.2.

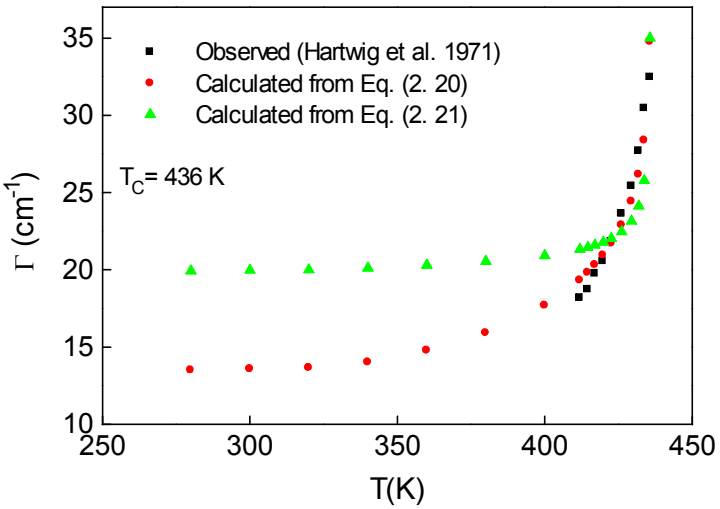

Figure 3.3.1 Damping constant calculated from Eqs. (2.20) and (2.21) as a function of temperature for the B_1 libration Raman mode of $NaNO_2$ (T_C= 436 K). The observed bandwidths of this mode are also plotted here (Hartwig *et al.* 1971).

Table 3.3.1 Values of the background bandwidth Γ_0 and the coefficient A (Eq. 2.20), and values of Γ_0' and A' (Eq. 2.21), for the B_1 libration Raman mode of $NaNO_2$ in the ferroelectric phase (436 K).

Crystal	Raman mode	$\Gamma_0(cm^{-1})$	$A(cm^{-1})$	$\Gamma_0'(cm^{-1})$	$A'(cm^{-1})$
$NaNO_2$	B_1 libration	13.0586	3.4127	19.6212	0.6356

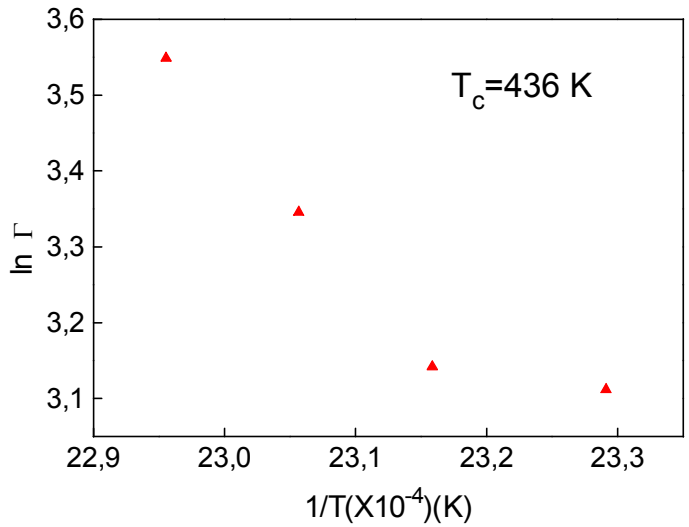

Figure 3.3.2 Plot of $\ln\Gamma$ vs $1/T$ (Arrhenius plot) for the B_1 libration Raman mode of $NaNO_2$ for the temperature interval indicated to calculate the activation energy according to Eq. (2. 23). (The damping constants used here, have been calculated from Eq. (2. 20)).

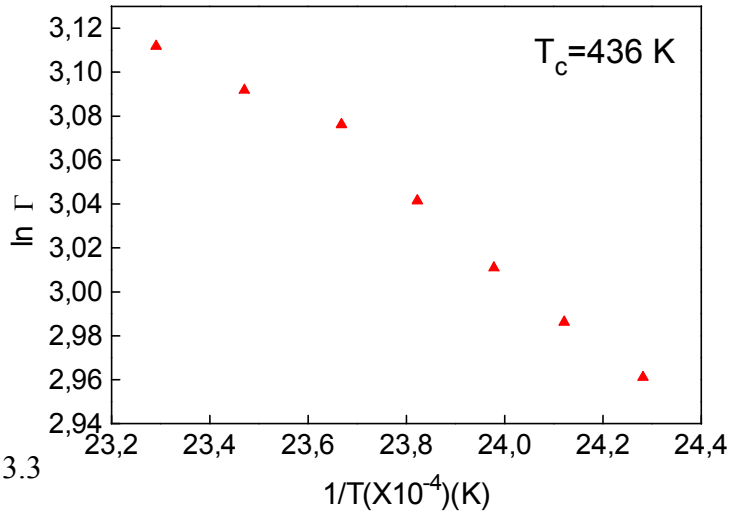

Figure 3.3.3 Plot of $\ln\Gamma$ vs $1/T$ (Arrhenius plot) for the B_1 libration Raman mode of $NaNO_2$ for the temperature interval indicated to calculate the activation energy according to Eq. (2. 23). (The damping constants used here, have been calculated from Eq. (2. 20)).

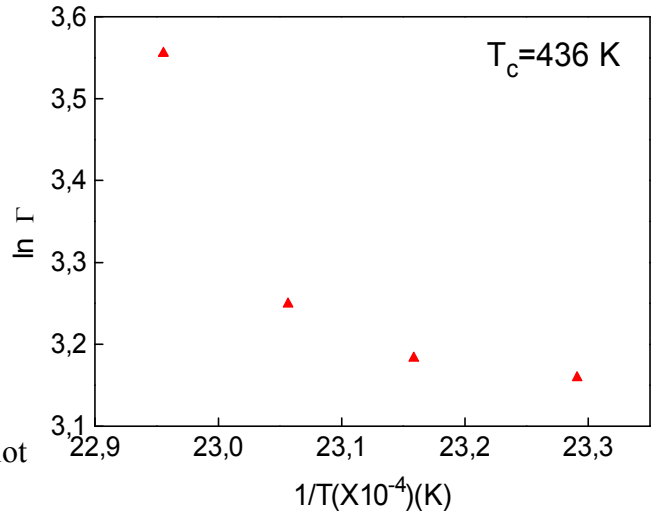

Figure 3.3.4 Plot of $\ln\Gamma$ vs $1/T$ (Arrhenius plot) for the B_1 libration Raman mode of $NaNO_2$ for the temperature interval indicated to calculate the activation energy according to Eq. (2. 23). (The damping constants used here, have been calculated from Eq. (2. 21)).

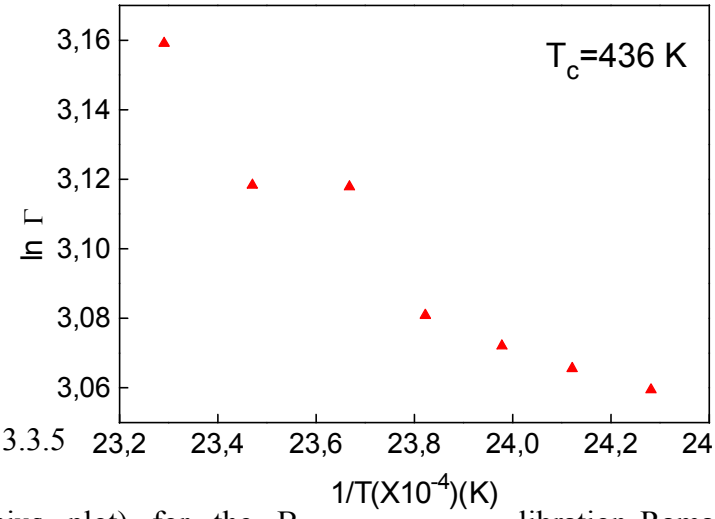

Figure 3.3.5 Plot of $\ln\Gamma$ vs $1/T$ (Arrhenius plot) for the B_1 libration Raman mode of $NaNO_2$ for the temperature interval indicated to calculate the activation energy according to Eq. (2. 23). (The damping constants used here, have calculated from Eq. (2. 21)).

Table 3.3.2 Values of the activation energy U calculated in the temperature interval for the B_1 libratinal Raman mode of $NaNO_2$ according to Eq. (2. 23) where the damping constant (Eqs. 2.20 and 2. 21) was used in the ferroelectric phase (T_C= 436 K).

Crystal	Raman mode	Damping Constant	Temperature range T(K)	Activation energy (eV)	k_BT_C (eV)
$NaNO_2$	B_1 libration	Eq. (2.20)	435.6 < T < 429.3	1.1480	0.0376
			429.3 < T < 411.8	0.1362	
		Eq. (2. 21)	435.6 < T < 429.3	0.9439	
			429.3 < T < 411.8	0.0852	

3.4 Calculation of the Damping Constant and the Activation Energy as a function of Temperature close to the Phase Transition Point for the Raman mode of A_2 libration in $NaNO_2$.

We evaluated the damping constant by using the values of the order parameter calculated from MFT, Eq. (2.16). We fitted Eqs. (2.20) and (2.21) to the observed Raman bandwidths for the A_2 libration mode of $NaNO_2$ (Hartwig *et al*. 1971) to evaluate the background constants Γ_0 and Γ_0', also the coefficients A and A' in Eqs. (2.20) and (2.21). These values have been found as Γ_0= 13.7919 cm^{-1}, A= 2.6388 cm^{-1}, Γ_0'= 17.7588 cm^{-1}, A'= 0.7197 cm^{-1}. We tabulated these values in Table 3.4.1. The observed Raman bandwidths (Hartwig *et al*. 1971) and the damping constants calculated by means of Eqs. (2.20) and (2.21) as a function of temperature for the A_2 libration Raman mode of $NaNO_2$ are plotted in Fig. 3.4.3.

We used Eq. (2.23) to calculate the activation energy of the A_2 libration Raman mode of $NaNO_2$. We represented the damping constant calculated at various temperatures in terms of an Arrhenius plot, Fig. 3.4.4. The slope of this graph gives us the activation energy and its value has been found as 0.5079 eV. The temperature range for this graph is from 435 K to 427.6 K. We also plotted this Arrhenius plot between the 427.6 K and 413.1 K in Fig. 3.4.5 and the slope of this graph gives us the activation energy as 0.1580 eV. The damping constants represented both in Fig. 3.4.4 and Fig. 3.4.5 have been calculated from Eq. 2.20. Likewise, these Arrhenius plots have been plotted for the same temperature region given above in Fig. 3.4.6 and Fig. 3.4.7 by representing the damping constants calculated from Eq. 2.21. The slopes of these graphs give us the activation energies as 0.5860 eV and 0.0775 eV, respectively. All these activation energy values have been given in Table 3.4.2.

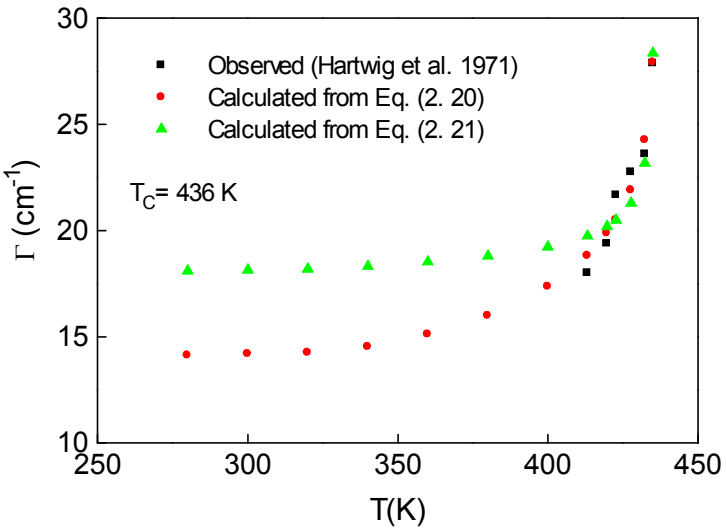

Figure 3.4.1 Damping constant calculated from Eqs. (2.20) and (2.21) as a function of temperature for the A_2 libration Raman mode for $NaNO_2$. The observed bandwidths of this mode are also plotted here (Hartwig *et al.* 1971).

Table 3.4.1 Values of the background bandwidth Γ_0 and the coefficient A (Eq. 2.20), and values of Γ_0' and A' (Eq. 2.21) for the A_2 libration Raman mode of $NaNO_2$ in the ferroelectric phase T_C= (436 K).

Crystal	Raman mode	$\Gamma_0(cm^{-1})$	$A(cm^{-1})$	$\Gamma_0'(cm^{-1})$	$A'(cm^{-1})$
$NaNO_2$	A_2 Libration	13.7919	2.6388	17.7588	0.7197

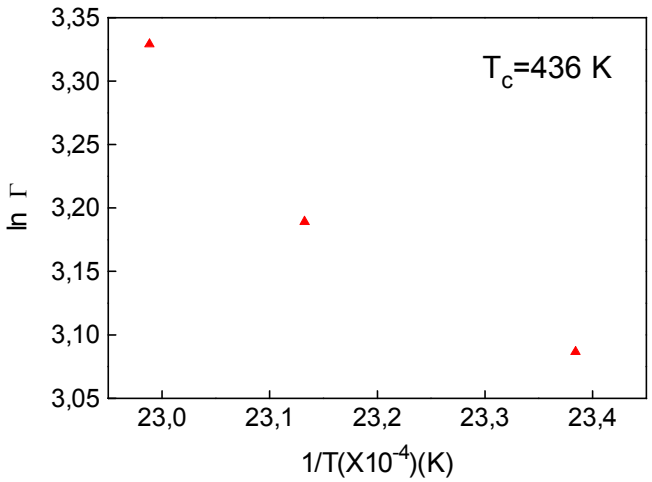

Figure 3.4.2 A plot of $\ln\Gamma$ vs $1/T$ (Arrhenius plot) for the A_2 libration Raman mode of $NaNO_2$ for the temperature interval indicated to calculate the activation energy according to Eq. (2. 23). (The damping constants used here, have been calculated from Eq. (2. 20)).

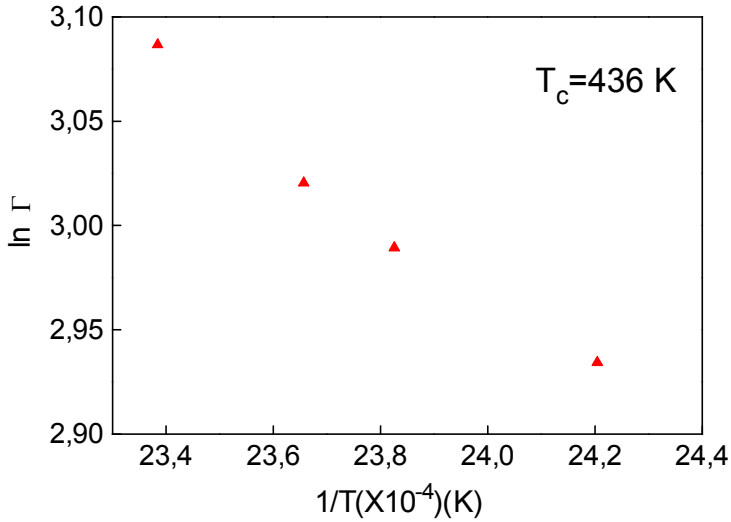

Figure 3.4.3 A plot of $\ln\Gamma$ vs $1/T$ (Arrhenius plot) for the A_2 libration Raman mode of $NaNO_2$ for the temperature interval indicated to calculate the activation energy according to Eq. (2. 23). (The damping constants used here, have been calculated from Eq. (2. 20)).

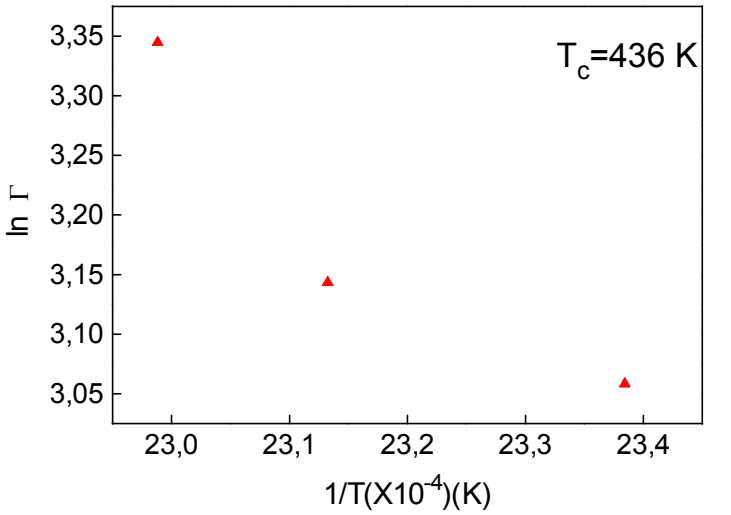

Figure 3.4.4 A plot of $\ln\Gamma$ vs $1/T$ (Arrhenius plot) for the A_2 libration Raman mode of $NaNO_2$ for the temperature interval indicated to calculate the activation energy according to Eq. (2. 23). (The damping constants used here, have been calculated from Eq. (2. 21)).

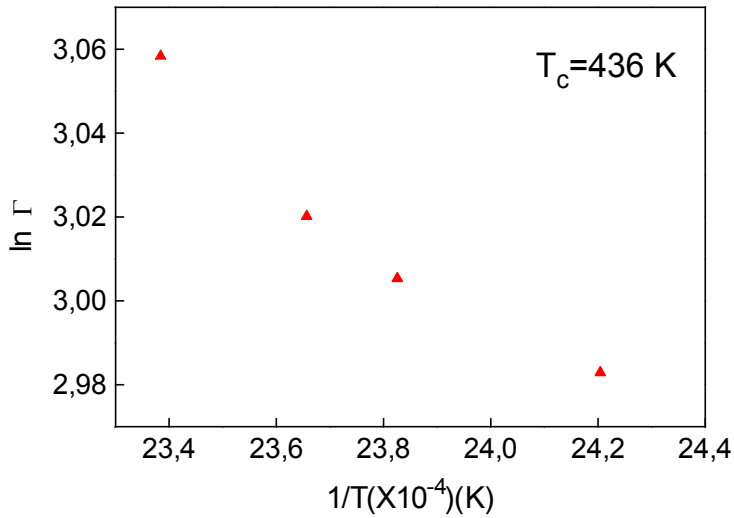

Figure 3.4.5 A plot of $\ln\Gamma$ vs $1/T$ (Arrhenius plot) for the A_2 libration Raman mode of $NaNO_2$ for the temperature interval indicated to calculate the activation energy according to Eq. (2. 23). (The damping constants used here, have been calculated from Eq. (2. 21)).

Table 3.4.2 Values of the activation energy U calculated in the temperature interval for the A_2 libratinal Raman mode of NaNO2 according to Eq. (2. 23) where the damping constant (Eqs. 2.20 and 2. 21) was used in the ferroelectric phase (T_C= 436 K).

Crystal	Raman mode	Damping Constant	Temperature range T(K)	Activation energy (eV)	k_BT_C (eV)
$NaNO_2$	A_2 libration	Eq. (2.20)	435 < T < 427.6	0.5079	0.0376
			427.6 < T < 413.1	0.1580	
		Eq. (2. 21)	435 < T < 427.6	0.5860	
			427.6 < T < 413.1	0.0775	

3.5 Calculation of the Order Parameter, Damping Constant and the Activation Energy as a function of Temperature in the Ferroelectric phase for $NaNO_2$.

The temperature dependence of the order parameter and order parameter squared are calculated by using MFT that is given by Eq. (2.16). The temperature range is from 329 K to 435.5 K and the critical temperature of $NaNO_2$ is 436 K (A. Da Costa Lamas *et al.* 1981). We plotted order parameter versus temperature graph in Fig. 3.5.1 and order parameter square versus temperature graph in Fig. 3.5.2.

The values of the order parameter calculated from Eq. (2.16) are used to compute the damping constant as a function of temperature on the basis of the soft phonon-hard phonon coupling model for $NaNO_2$ in the ferroelectric phase. In Fig. 3.5.3, we plotted damping constant calculated from Eq. (2.20) and Eq. (2.21) as a function of temperature for the ferroelectric mode of $NaNO_2$.

By representing the damping constant calculated at various temperatures in terms of an Arrhenius plot, we calculated the activation energy. In Fig. 3.5.4, we plotted $\ln\Gamma$ versus $\frac{1}{T}$ graph (Arrhenius plot) and the slope of this graph gives us the activation energy as 0.9811 eV. Here, the damping constant values have been calculated from Eq. (2.20) and the temperature range is from 421.1 K to 435.5 K. Similarly, we plotted $\ln\Gamma$ versus $\frac{1}{T}$ graph (Arrhenius plot) In Fig. 3.5.4, by representing the damping constant calculated from Eq. (2.21). Here, the temperature range is also from 421.1 K to 435.5 K and the slope of this graph gives us the activation energy as 1.7645 eV. These activation energy values have been tabulated in Table 3.5.1.

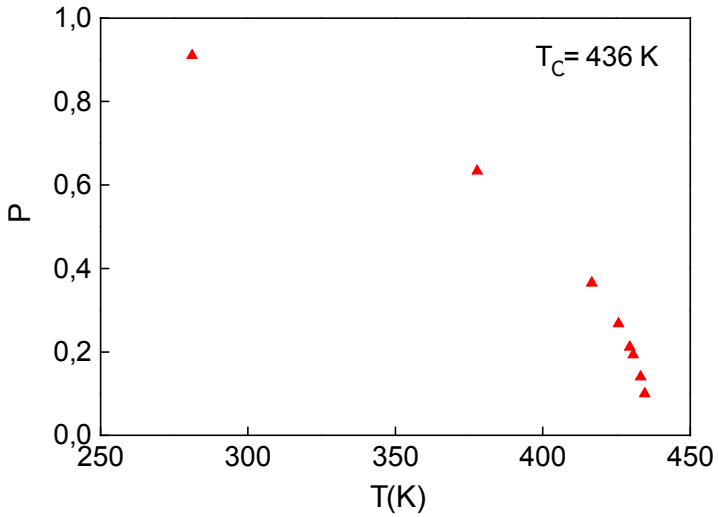

Figure 3.5.1 Order parameter, P, as a function of temperature for ferroelectric phase in $NaNO_2$ according to Eq.(2.16) from the molecular field theory.

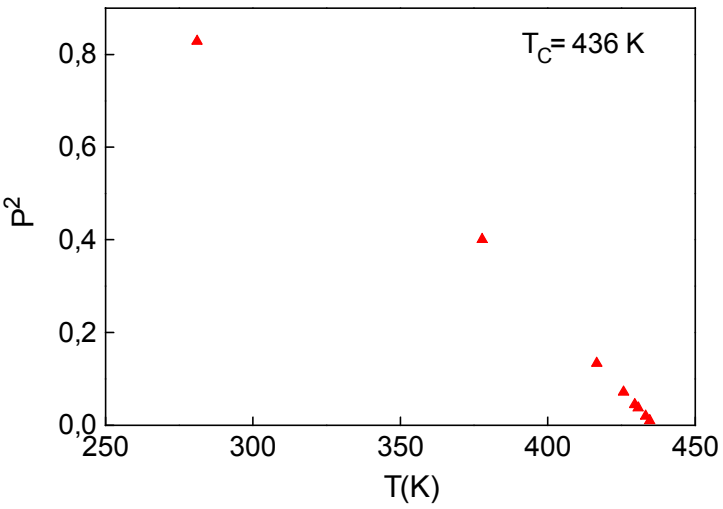

Figure 3.5.2 Order parameter squared, P^2, as a function of temperature for ferroelectric phase in $NaNO_2$ according to Eq.(2.16) from the molecular field theory.

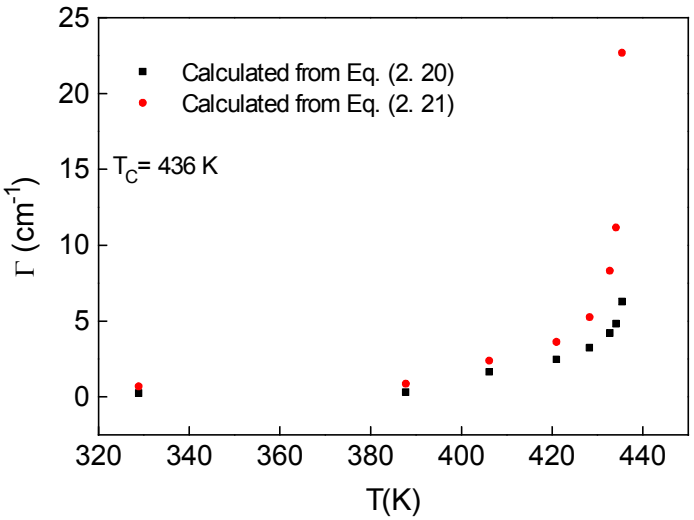

Figure 3.5.3 Damping constant calculated from Eqs. (2.20) and (2.21) as a function of temperature for ferroelectric phase in $NaNO_2$.

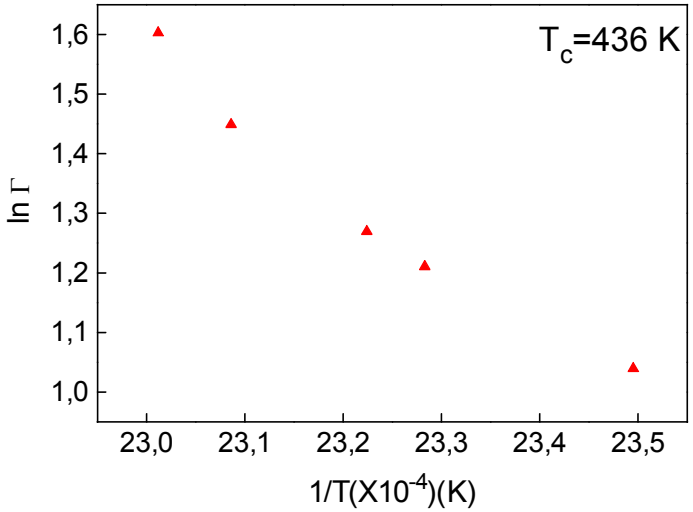

Figure 3.5.4 A plot of $\ln\Gamma$ vs $1/T$ (Arrhenius plot) for the ferroelectric phase in $NaNO_2$ to calculate the activation energy according to Eq. (2. 23). (The damping constants used here, have been calculated from Eq. (2. 20)).

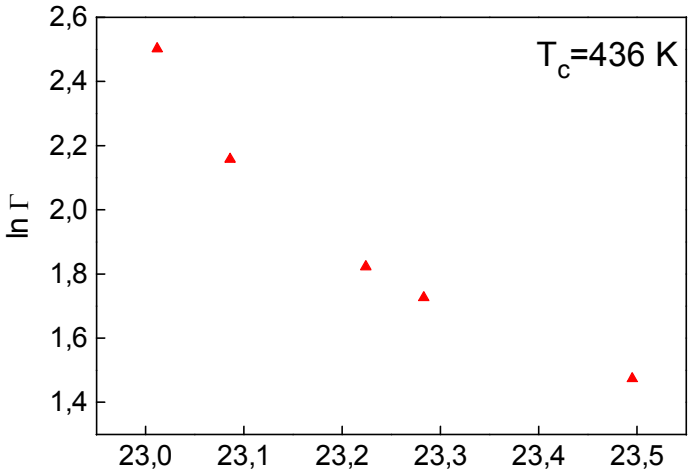

Figure 3.5.5 A plot of $\ln\Gamma$ vs $1/T(X10^{-4})(K)$ $1/T$ (Arrhenius plot) for ferroelectric phase in $NaNO_2$ to calculate the activation energy according to Eq. (2. 23). (The damping constants used here, have been calculated from Eq. (2. 21)).

Table 3.5.1 Values of the activation energy U calculated in the temperature interval for the ferroelectric phase of $NaNO_2$ according to Eq. (2. 23) where the damping constant (Eqs. 2.20 and 2. 21) was used in the ferroelectric phase (T_C= 436 K).

Crystal	Damping Constant	Temperature range T(K)	Activation energy (eV)	k_BT_C (eV)
$NaNO_2$	Eq. (2.20)	421.1 < T < 435.5	0.9811	0.0376
	Eq. (2. 21)	421.1 < T < 435.5	1.7645	

3.6 Calculation of the Order Parameter, Damping Constant and the Activation Energy as a function of Temperature close to the Phase Transition Point for the Raman mode of υ_1 in $(NH_4)_2SO_4$.

The temperature dependence of the order parameter, given by Eq. (2.16), is used to calculate the order parameter. The temperature range for this mode is from

10.5 K to 176 K (Z. Iqbal and C. W. Christoe 1976) and the critical temperature of $(NH_4)_2SO_4$ is 223 K (Mathias and Remeika 1956). We extrapolated the temperature from 176 K to 220 K. We plotted order parameter versus temperature graph in Fig. 3.6.1 and also we plotted the order parameter squared versus temperature graph in Fig. 3.6.2.

We used the order parameter values calculated from MFT, Eq. (2.16), to compute the damping constant as a function of temperature for the υ_1 mode in $(NH_4)_2SO_4$. We fitted Eqs. (2.20) and (2.21) to the observed Raman bandwidths (Z. Iqbal and C. W. Christoe 1976) to find the background constants Γ_0, Γ_0' and the coefficients A and A' in Eqs. (2.20) and (2.21). We have found the following values for the constants, $\Gamma_0 = 27.2510$ cm^{-1}, $A = 90.8156$ cm^{-1}, $\Gamma_0' = 26.310$ cm^{-1} and $A' = 27.2232$ cm^{-1}. The observed Raman bandwidths and the damping constants calculated from Eq. (2.20) and Eq. (2.21) as a function of temperature for the υ_1 Raman mode in $(NH_4)_2SO_4$ are plotted in Fig. 3.6.3.

We calculated the activation energy by representing the damping constant at various temperatures in terms of Arrhenius plots. In Fig. 3.6.4, we plotted $\ln\Gamma$ versus $\frac{1}{T}$ graph and the slope of this graph gives us the activation energy as 0.1990 eV. Here, we used the damping constant calculated from eq. (2. 20). Similarly, we plotted $\ln\Gamma$ versus $\frac{1}{T}$ graph in Fig. 3.6.5 by using the damping constant calculated from Eq. (2. 21) and we found the activation energy as 0.2285 eV. The temperature range for these two graphs is from 205 K to 220 K. We tabulated these activation energy values in Table 3.6.2.

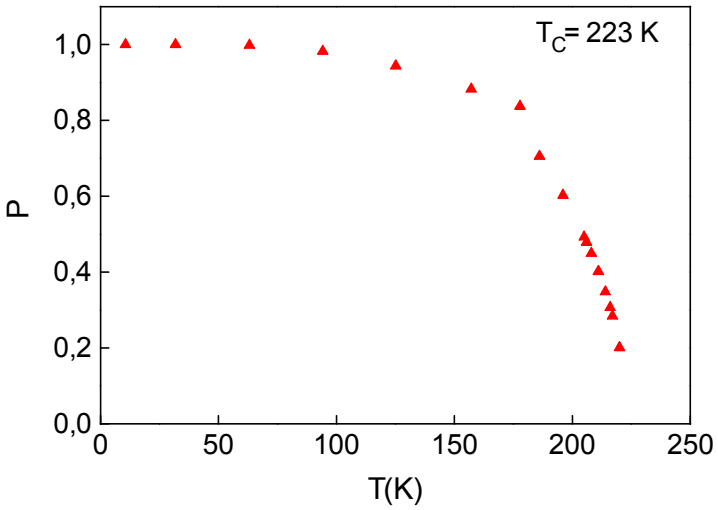

Figure 3.6.1 Order parameter, P, as a function of temperature for $(NH_4)_2SO_4$ according to Eq.(2.16) from the molecular field theory.

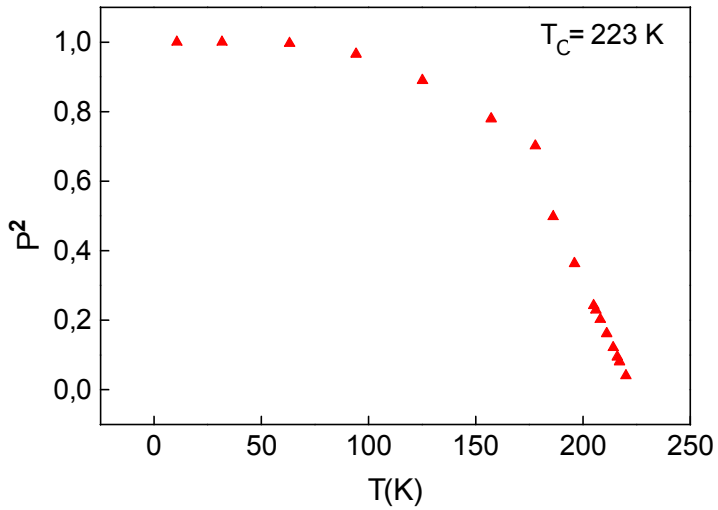

Figure 3.6.2 Order parameter squared,P^2, as a function of temperature for $(NH_4)_2SO_4$ according to Eq.(2.16) from the molecular field theory.

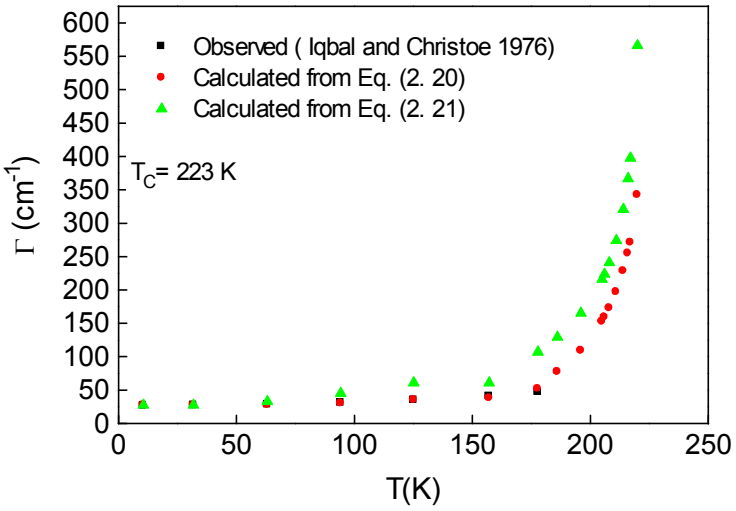

Figure 3.6.3 Damping constant calculated from Eqs. (2.20) and (2.21) as a function of temperature for the υ_1 Raman mode for $(NH_4)_2SO_4$. The observed bandwidths of this mode are also plotted here (Z. Iqbal and C. W. Christoe 1976).

Table 3.6.1 Values of the background bandwidth Γ_0 and the coefficient A (Eq. 2.20), and values of Γ_0' and A' (Eq. 2.21) for the υ_1 Raman mode of $(NH_4)_2SO_4$ in the ferroelectric phase (T_C= 223 K).

Crystal	Raman mode	$\Gamma_0(cm^{-1})$	$A(cm^{-1})$	$\Gamma_0'(cm^{-1})$	$A'(cm^{-1})$
$(NH_4)_2SO_4$	υ_1	27.2510	90.8156	26.310	27.2232

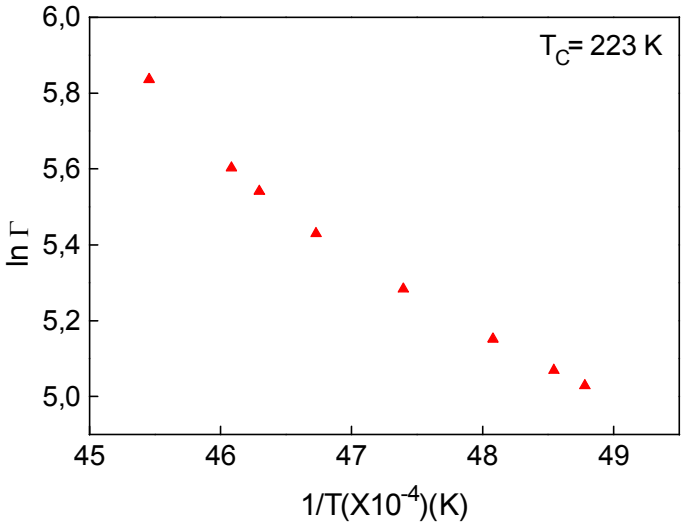

Figure 3.6.4 A plot of $\ln\Gamma$ vs $1/T$ (Arrhenius plot) for the υ_1 Raman mode of $(NH_4)_2SO_4$ for the temperature interval indicated to calculate the activation energy according to Eq. (2. 23).(The damping constants used here, have been calculated from Eq. (2. 20)).

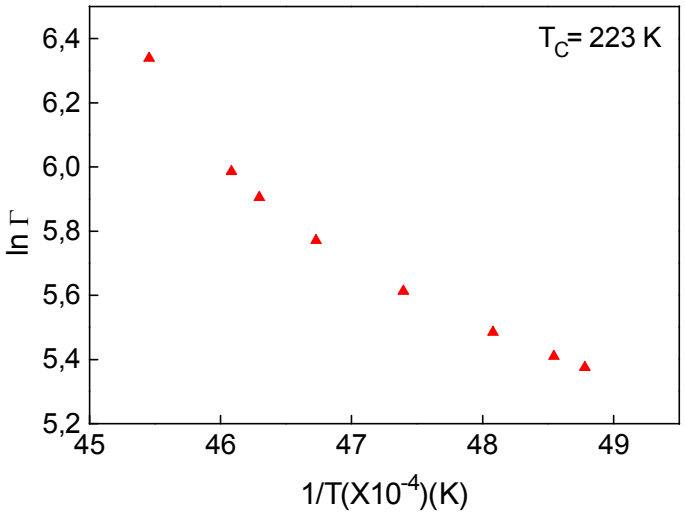

Figure 3.6.5 A plot of $\ln\Gamma$ vs $1/T$ (Arrhenius plot) for the υ_1 Raman mode of $(NH_4)_2SO_4$ for the temperature interval indicated to calculate the activation energy according to Eq. (2. 23). (The damping constants used here, have been calculated from Eq. (2. 21)).

Table 3.6.2 Values of the activation energy U calculated in the temperature interval for the υ_1 Raman mode of $(NH_4)_2SO_4$ according to Eq. (2. 23) where the damping constant (Eqs. 2. 20 and 2. 21) was used in the ferroelectric phase (T_C= 223 K).

Crystal	Raman mode	Damping Constant	Temperature range T(K)	Activation energy (eV)	k_BT_C (eV)
$(NH_4)_2SO_4$	υ_1	Eq. (2.20)	205< T < 220	0.1990	0.0192
		Eq. (2. 21)	205 < T < 220	0.2285	

3.7 Calculation of the Damping Constant and the Activation Energy as a function of Temperature close to the Phase Transition Point for the 364 cm^{-1} Raman librationl mode in $(NH_4)_2SO_4$.

We used the order parameter values calculated from Eq. (2. 16) to evaluate the damping constant as a function of temperature for the 364 cm^{-1} librational Raman mode in $(NH_4)_2SO_4$. The background constants Γ_0, Γ_0' and the coefficients A and A' have been found by fitting Eq. (2. 20) and Eq. (2. 21) to the observed Raman bandwitdhs (Z. Iqbal and C. W. Christoe 1976). We found, Γ_0=7.2913 cm^{-1}, Γ_0'=6.5816 cm^{-1}, A=181.4339 cm^{-1} and A'=35.7140 cm^{-1}. The damping constants calculated from Eqs. (2. 20) and (2. 21) and the observed Raman bandwitdhs (Z. Iqbal and C. W. Christoe 1976) as a function of temperature for the 364 cm^{-1} librational mode in $(NH_4)_2SO_4$ are plotted in Fig. 3.7.3.

By representing the damping constant at various temperatures in terms of Arrhenius plot, we calculated the activation energy of this mode. we plotted $\ln\Gamma$

versus $\frac{1}{T}$ graph in Fig. 3.7.4 and the slope of this graph gives us the activation energy as 0.2285 eV. The damping constant in $\ln\Gamma$ has been calculated by using Eq. (2. 20). Likewise, by representing the damping constant calculated from Eq. (2. 21), we plotted the same graph in Fig. 3.7.5 and slope of this graph gives us the activation energy as 0.2455 eV. The temperature range for these two graphs are from 205 K to 220 K. These activation energy values are tabulated in Table 3.7.2.

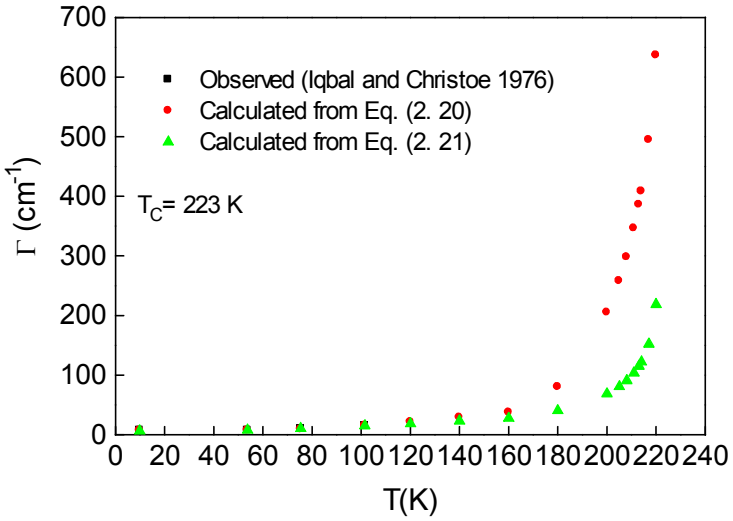

Figure 3.7.1 Damping constant calculated from Eqs. (2.20) and (2.21) as a function of temperature for the 364 cm^{-1} librational Raman mode for $(NH_4)_2SO_4$. The observed bandwidths of this mode are also plotted here (Z. Iqbal and C. W. Christoe 1976).

Table 3.7. 1 Values of the background bandwidth Γ_0 and the coefficient A (Eq. 2.20), and values of Γ_0' and A' (Eq. 2.21), for the 364 cm^{-1} librational Raman mode of $(NH_4)_2SO_4$ in the ferroelectric phase (223 K).

Crystal	Raman mode	$\Gamma_0(cm^{-1})$	$A(cm^{-1})$	$\Gamma_0'(cm^{-1})$	$A'(cm^{-1})$
$(NH_4)_2SO_4$	364 cm^{-1} libration	7.2913	181.4339	6.5816	35.7140

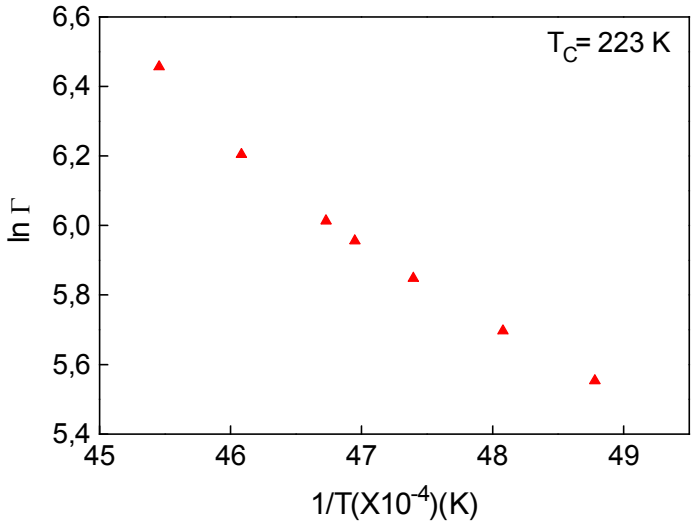

Figure 3.7.2 A plot of $\ln\Gamma$ vs $1/T$ (Arrhenius plot) for the 364 cm^{-1} librational Raman mode of $(NH_4)_2SO_4$ for the temperature interval indicated to calculate the activation energy according to Eq. (2. 23). (The damping constants used here, have been calculated from Eq. (2. 20)).

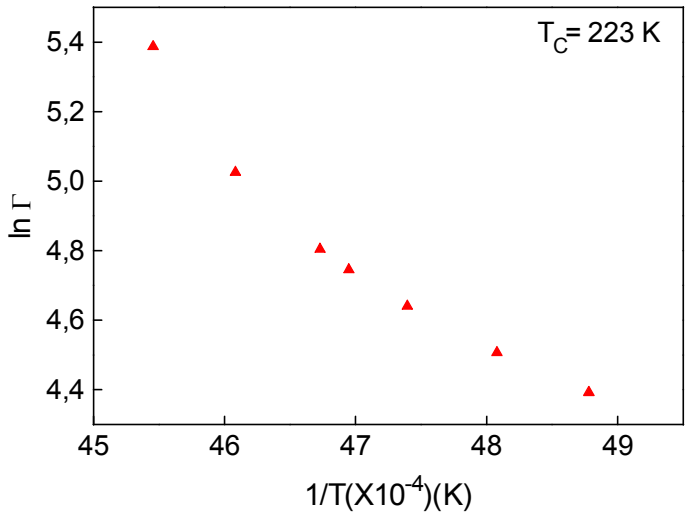

Figure 3.7.3 A plot of $\ln\Gamma$ vs $1/T$ (Arrhenius plot) for the 364 cm^{-1} librational Raman mode of $(NH_4)_2SO_4$ for the temperature interval indicated to calculate the activation energy according to Eq. (2. 23). (The damping constants used here, have been calculated from Eq. (2. 21)).

Table 3.7.2 Values of the activation energy U calculated in the temperature interval for the 364 cm^{-1} librational Raman mode of $(NH_4)_2SO_4$ according to Eq. (2. 23) where the damping constant (Eqs. 2.20 and 2. 21) was used in the ferroelectric phase (T_C= 223 K).

Crystal	Raman mode	Damping Constant	Temperature range T(K)	Activation energy (eV)	k_BT_C (eV)
$(NH_4)_2SO_4$	364 cm^{-1} libration	Eq. (2.20)	205 < T < 220	0.2285	0.0192
		Eq. (2. 21)	205< T < 220	0.2455	

3.8 Calculation of the Damping Constant and the Activation Energy as a function of Temperature close to the Phase Transition Point for the 394 cm^{-1} Raman librationl mode in $(NH_4)_2SO_4$.

We used the order parameter values calculated from Eq. (2. 16) to evaluate the damping constant as a function of temperature for the 394 cm^{-1} librational Raman mode in $(NH_4)_2SO_4$. We fitted Eq. (2. 20) and Eq. (2. 21) to the observed Raman bandwidths (Z. Iqbal and C. W. Christoe 1976) to find the background constants Γ_0, Γ_0' and the coefficients A and A'. These values are, Γ_0=7.3019 cm^{-1}, Γ_0'=6.5155 cm^{-1}, A=32.7723 cm^{-1} and A'=12.8709 cm^{-1}. The observed Raman bandwidths (Z. Iqbal and C. W. Christoe 1976) and the damping constants calculated from Eqs. (2. 20) and (2. 21) as a function of temperature for the 394 cm^{-1} librational mode in $(NH_4)_2SO_4$ are plotted in Fig. 3.8.3.

By representing the damping constant at various temperatures in terms of Arrhenius plot, we calculated the activation energy of this mode. . In Fig. 3.8.4, we plotted $\ln\Gamma$ versus $\frac{1}{T}$ graph and the slope of this graph gives us the activation energy as 0.2062 eV. The damping constant used in this graph is computed by using Eq. (2. 20). Similarly, by representing the damping constant calculated from Eq. (2. 21), we plotted $\ln\Gamma$ versus $\frac{1}{T}$ graph in Fig. 3.8.5 and the slope of this graph gives us the activation energy as 0.2447 eV. The temperature range for both two graphs is from 205 K to 220 K. We tabulated these activation energy values in Table 3.8.2.

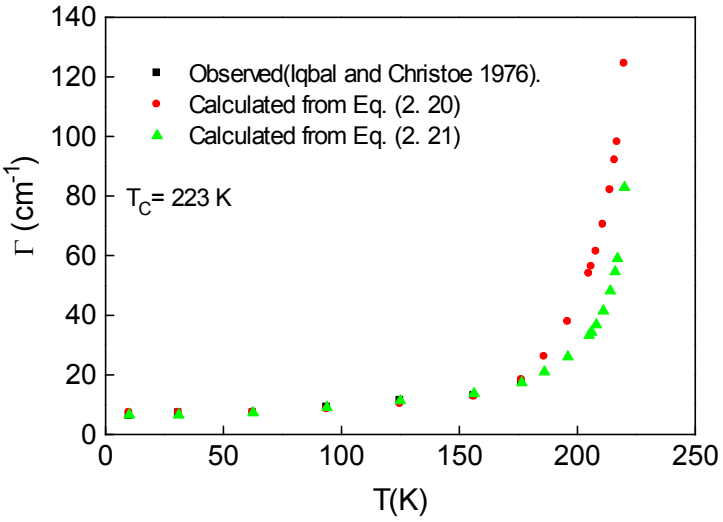

Figure 3.8.1 Damping constant calculated from Eqs. (2.20) and (2.21) as a function of temperature for the 394 cm^{-1} librational Raman mode for $(NH_4)_2SO_4$. The observed bandwidths of this mode are also plotted here (Z. Iqbal and C. W. Christoe 1976).

Table 3.8.1 Values of the background bandwidth Γ_0 and the coefficient A (Eq. 2.20), and values of Γ_0' and A' (Eq. 2.21), for the 394 cm^{-1} librational Raman mode of $(NH_4)_2SO_4$ in the ferroelectric phase (223 K).

Crystal	Raman mode	$\Gamma_0(cm^{-1})$	$A(cm^{-1})$	$\Gamma_0'(cm^{-1})$	$A'(cm^{-1})$
$(NH_4)_2SO_4$	394 cm^{-1} libration	7.3019	32.7723	6.5155	12.8709

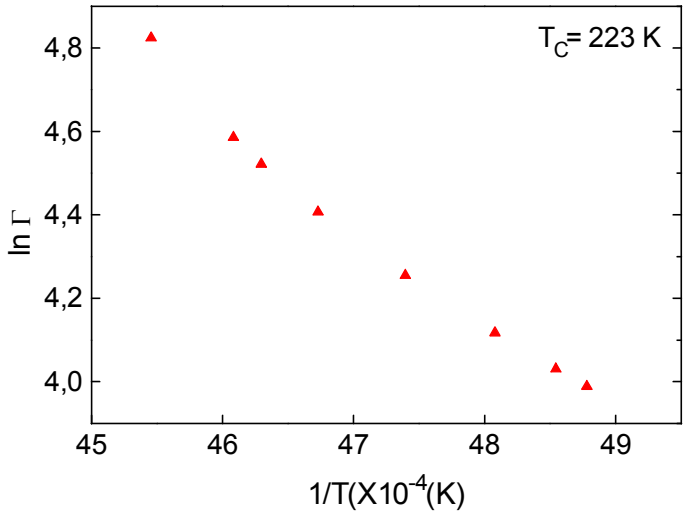

Figure 3.8.2 A plot of $\ln\Gamma$ vs $1/T$ (Arrhenius plot) for the 394 cm^{-1} librational Raman mode of $(NH_4)_2SO_4$ for the temperature interval indicated to calculate the activation energy according to Eq. (2. 23). (The damping constants used here, have been calculated from Eq. (2. 20)).

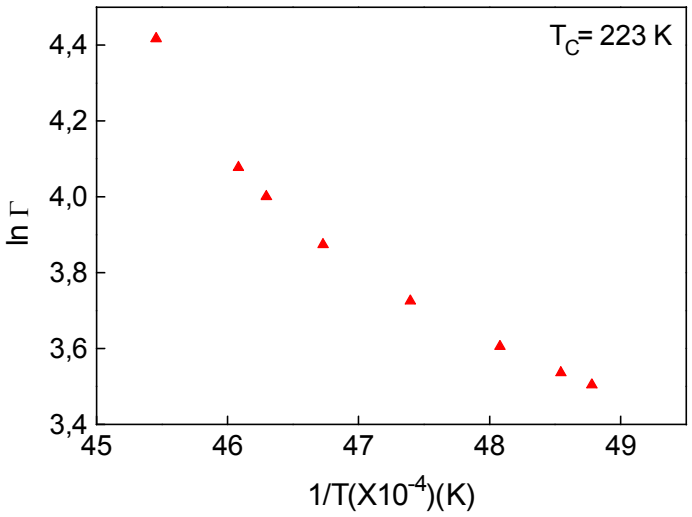

Figure 3.8.3 A plot of $\ln\Gamma$ vs $1/T$ (Arrhenius plot) for the 394 cm^{-1} librational Raman mode of $(NH_4)_2SO_4$ for the temperature interval indicated to calculate the activation energy according to Eq. (2. 23). (The damping constants used here, have been calculated from Eq. (2. 21)).

Table 3.8.2 Values of the activation energy U calculated in the temperature interval for the 394 cm^{-1} librational Raman mode of $(NH_4)_2SO_4$ according to Eq. (2. 23) where the damping constant (Eqs. 2.20 and 2. 21) was used in the ferroelectric phase (T_C= 223 K).

Crystal	Raman mode	Damping Constant	Temperature range T(K)	Activation energy (eV)	k_BT_C (eV)
$(NH_4)_2SO_4$	394 cm^{-1} libration	Eq. (2.20)	205 < T < 220	0.2062	0.0192
		Eq. (2. 21)	205 < T < 220	0.2447	

DISCUSSION

The order parameter and order parameter square were calculated by using Eq. (2. 16), derived from molecular field theory for $NaNO_2$ and $(NH_4)_2SO_4$ in the ferroelectric phase in $NaNO_2$. The temperature dependence of the order parameter has been plotted in Fig. 3.1.1 for $NaNO_2$ and Fig. 3.6.1 for $(NH_4)_2SO_4$. From these figures we see that, at very low temperatures the order parameter is namely 1 (ordered ferroelectric phase) and near the critical temperature the orderparameter goes to zero (disordered paraelectric phase) and as the temperature increases the order parameter decreases.

By using the temperature dependence of the order parameter derived from molecular field theory (Matsushita, 1976), we calculated the damping constants for the Raman modes by means of Eqs. (2. 20) and (2. 21). Then we connected the theoretical results with the experimental ones. We were restricted ourselves to the experimental data points in our plots since there were not many experimental data to calculate the damping constants for the modes in $NaNO_2$ and $(NH_4)_2SO_4$. We extrapolated the temperature for all the modes that we studied here. We calculated the background constants Γ_0, Γ_0' and the coefficients, A and A' in Eqs. (2. 20) and (2. 21) with help of the damping constant versus temperature graphs. We tabulated these values in Tables 3.1.1, 3.2.1, 3.3.1, 3.4.1, 3.6.1, 3.7.1, and 3.8.1. Our figures show that as the temperature increases the damping constant also increases but near the

critical temperature, 436 K for $NaNO_2$ and 223 K for $(NH_4)_2SO_4$, there is an anomalous behaviour of the damping constant. Our plots show that the calculated data for the damping constants are in good agreement with the observed Raman bandwidths for all the modes in $NaNO_2$ and $(NH_4)_2SO_4$. The damping constant which depended upon the square of the spontaneous polarization logarithmically (Eq. 2.20) agreed with the observed bandwidths, as shown in Figs. 3.1.3, 3.2.1, 3.3.1, 3.4.1, 3.6.3, 3.7.1, and 3.8.1. So, the temperature dependence of the damping constant which depended upon the square of the spontaneous polarization to the power 1/2 (Eq. 2.21), was not very satisfactory in comparison with the observed bandwidths. We also plotted the damping constant versus temperature graph for the ferroelectric phase of $NaNO_2$ to predict the behaviour of the damping constant. We did not find the background constant and the coefficients of this mode since there is no experimental data available.

By representing the damping constant calculated at various temperatures in terms of Arrhenius plots, we evaluated the activation energies of all modes of $NaNO_2$ and $(NH_4)_2SO_4$ by using Eq. (2. 23). We used the damping constants given by Eqs. (2. 20) and (2. 21) seperately to calculate the activation energy of each mode. We tabulated the activation energy values for all the modes in Tables 3.1.2, 3.2.2, 3.3.2, 3.4.2, 3.5.2, 3.6.2, 3.7.2, and 3.8.2. The activation energies we obtained for all the Raman modes of $NaNO_2$ and $(NH_4)_2SO_4$, are much larger than the value of $k_BT = 0.0376\ eV$ (for $NaNO_2$) , $k_BT = 0.0192\ eV$ (for $(NH_4)_2SO_4$) which indicates that these crystals undergo an order-disorder type phase transition, as also indicated for the $LiNH_4SO_4$ crystal (Hossain *et al*. 1994). We observed that as the temperature is well away from the critical temperature, the activation energy decreases.

CONCLUSIONS

We investigated the temperature dependence of the order parameter, damping constant and the activation energy of the modes of $NaNO_2$ and $(NH_4)_2SO_4$. We observed that as the temperature increases the order parameter decreases. As the temperature increases, the damping constant increases for the B_1 asymmetric, B_2 libration, B_1 libration, A_2 asymmetric in $NaNO_2$, and υ_1, 364 cm^{-1} libration and 394 cm^{-1} libration modes in $(NH_4)_2SO_4$. The calculated damping constants for the modes in both $NaNO_2$ and $(NH_4)_2SO_4$ are in good agreement with the observed Raman bandwidths. Thus, we predict the critical behaviour of the damping constant exhibited by the $NaNO_2$ and $(NH_4)_2SO_4$ crystals near the transition temperature in the ferroelectric phase.

Finally, we computed the activation energy of all the modes that we studied for $NaNO_2$ and $(NH_4)_2SO_4$. We obtained that as the temperature increases toward the critical temperatures, the activation energy also increases.

REFERENCES

Abe, R., and Shibata, N. 1977. A microscopic model for the ferroelectric phase transition in $(NH_4)_2SO_4$. *J. Phys. Soc. Jap. 43: 1308.*

Asawa, C. K., and Barnoski, K. 1970. Raman spectra and mode frequency shifts of ferroelectric sodium nitrite at 77 and 294 K. *Phys. Rev. B 2: 205.*

Axe, J. D. 1968. Infrared dielectric dispersion and apparent ionic charges in sodium nitrite. *Phys. Rev. 167: 573.*

Badr, Y. A., and Awad, S. 1984. On the low temperature phase transition in $(NH_4)_2SO_4$. *J. Phys. Chem. Solids 45: 351.*

Barnoski, M. K., and Ballantyne, J. M. 1968. Temperature- dependent vibrational modes in sodium nitrite. *Phys. Rev. 174: 946.*

Bartoli, F. F., and Litovitz, T. A. 1972. Raman scattering: orientational motions in liquids. . *J. Chem. Phys. 56: 413.*

Becucci, M., and Castellucci E. 1989. Relaxation dynamics of phonons in $NaNO_2$ by means of high-resolution Raman linewidth measurement. *Chem. Phys. 135: 363.*

Berg, R. W., Kerridge, D. H., and Larsen, P. H. 2006. $NaNO_2$ + $NaNO_3$ Phase diagram: new data from DSC and Raman spectroscopy. *J. Chem. Eng. Data. 51: 34.*

Blinc, R., and Levstek, I. 1960. NMR and IR of $(NH_4)_2SO_4$ and $(NH_4)_2BeF_4$. *J. Phys. Chem. Solids 12: 295.*

Blinc, R., and Zeks, B. 1974.Soft modes in Ferroelectrics and Antiferroelectrics. North Holland, Amsterdam.

Blinc, R., Mali, M., Osredkar R., Prelesnik A., Seliger, J., and Zupancic, I. 1972. ^{14}N quadrupole coupling in paraelectric $(NH_4)_2SO_4$. *Chem. Phys. Lett. 14: 49.*

Brehat, F., and Wyncke, B. J. 1985. Analysis of the temperature-dependent lattice modes in sodium nitrite by infrared spectroscopy. *J. Phys. C: Solid State Phys. 18: 1705.*

Buchheit, W., Herth, G., and Peterson J. 1981. Study of commensurate and incommensurate phases in $NaNO_2$ by 23Na NMR. *Solid State Comm. 40: 411.*

Chiba, T. 1962. Deuteron magnetic resonance study of several deuterated ammonium salts. *J. Chem. Phys. 36: 1122.*

Chisler, E. V., and Shur, M. S. 1966. The Raman spectrum of $NaNO_2$ in the ferroelectric phase. *Phys. Stat. Solidi. 17: 163.*

Chisler, E. V., and Shur, M. S. 1967. Study of ferroelectric transition in $NaNO_2$ using Raman scattering spectrum in the region of NO_2 anion vibrations. *Phys. Sov. Solid State. 9: 796.*

Cummins, H. Z. 1990. Experimental studies of structurally incommensurate crystal phases. *Phys. Rept. 185: 211.*

Da Costa Lamas, A., Chang, S. L., and Caticha-Ellis, S. 1981. On the use of powder diffractometry in the study of phase transitions, case of $NaNO_2$. *Phys. Stat. sol. (a) 68: 173.*

Dahlborg, U., Larsson, K. E., and Pirkmajer, E. 1970. Rotational motions in solids the ferroelectric transition in $(NH_4)_2SO_4$, studied by cold neutrons. *Physica 49: 1*

Durand, D., Bernard, L., Mezei, F., Currat, R., Denoyer, F., and Lambert, M. 1986. Incommensurate phase transition in sodium nitrite: A study of the dynamics by neutron spin scho technique. *Physica B. 136: 325.*

Durand, D., Denoyer, F., Lampert, M., Bernard L., Currat R. 1982. Etude par rayons X et par neutrons de la phase incommensurable du nitrite de sodium *J. Phys. France. 43: 149.*

Ehrhardt, K. D., and Michel, K. H. 1981. Microscopic model of $NaNO_2$ based on reorientations and translations. *Z. Phys.Rev.Lett. 46: 291.*

Ehrhardt, K. D., and Michel, K. H. 1981. Microscopic model of $NaNO_2$ in the paraelectric phase. *Z. Phys. B. Condensed Matter. 41: 329.*

El-Korashy, A., El-Zahed, H., and Radwan, M. 2003. Optical studies of $(NH_4)_2SO_4$ single crystal in the paraelectric phase. *J. Phys. Chem. Solids 64: 2141.*

Ema, K., Hamano, K., and Hatta, I. 1975. Study of thermal expansion of $NaNO_2$ with special emphasis on the vicinity of the transition points. *J. Phys. Soc. Jap. 39: 726.*

Enginer, Y., Salihoğlu, S., and Yurtseven, H. 2003. Temperature dependence of susceptibity in the ferrielectric phase of ammonium sulphate. *Chin. J. Phys. 41: 4.*

Esayan, S. K., Lemanov, V. V., and Mamatkulov, N. 1981. Ultrasonic investigations of phase transitions in $NaNO_2$ crystals. *Sov. Phys. Solid State. 23: 1195.*

Fahim, M. A. 2000. A detailed IR study of the order-disorder phase transition of $NaNO_2$. *Thermochimica Acta. 363: 121.*

Fivez, J., and Michel, K. 1983. Dynamics of $NaNO_2$ in the paraelectric and in the incommensurate phase. *Z. Phys. B. Condensed Matter. 51: 127.*

Fujimoto, M., Dressel, L. A., and Yu, T. J. 1977. Phase transition in ammonium sulphate at -50 ^{o}C; A study of librational mode softening by paramagnetic NH_3^+ probes. *J. Phys. Chem. Solids 38: 97.*

Grecu, M. N., Constantinescu, S., and Grecu, V. V. 2003. Recent results of EPR and Mössbauer investigations on lattice dynamics in ammonium sulphate. *Rom. Rep. Phys. 55: 130.*

Hamono, K. 1964. Dielectric and electrostrictive anomalies slightly above the curie point of NaNO2. *J. Phys. Soc. Jap. 19: 945.*

Hamano, K., and Ema, K. 1978. Critical behaviour of adiabatic and isothermal elastic compliances of $NaNO_2$. *J. Phys. Soc. Jap. 45: 923.*

Hasebe, K. 1981. Studies of the crystal of ammonium sulfate in connection with its ferroelectic phase transition. *J. Phys. Soc. Jap. 50: 1266.*

Hasebe, K. 1981. Phase transition in ammonium sulfate. *J. Phys. Soc. Jap. 50: 2660.*

Hasebe, K., and Tanisaki, S. 1977. X-Ray diffuse scattering of paraelectric ammonium sulfate. *J. Phys. Soc. Jap. 42: 568.*

Hartwig, C. M., Wiener-Avnear, E., and Porto, S. P. S. 1972. Analysis of the temperature-dependent phonon structure in sodium nitrite by raman spectroscopy. *Phys. Rev. B. 5: 79*

Hatta, I. 1984. Ultrasonic Study of $NaNO_2$. III. Critical behaviour of elastic stiffness constants at the normal-to-incommensurate phase transition. *J. Phys. Soc. Jap. 53: 635.*

Hatta, I., Hanami, M., and Hamano, K. 1980. Ultrasonic study of $NaNO_2$. II. Dynamics of amplitude mode in incommensurate phase. *J. Phys. Soc. Jap. 48: 160.*

Hatta, I., Shimizu, Y., and Hamano, K. 1978. Ultrasonic study of $NaNO_2$. I. Anisotropic character of elastic constant and attenuation coefficients. *J. Phys. Soc. Jap. 44: 1887.*

Hoshino, S. 1964. An evidence for existance of a Third phase in $NaNO_2$. *J. Phys. Soc. Jap. 19: 140.*

Hoshino, S., and Motegi, H. 1967. X- ray Study on the phase transition of $NaNO_2$. *J. Phys. Soc. Jap. 6: 708.*

Hoshino, S., Vedam, K., Okaya Y., and Pepinsky, R. 1958. Dielectric and thermal study of $(NH_4)_2SO_4$ and $(NH_4)_2BeF_4$ transitions. *Phys. Rev. 112: 405.*

Ikeda, T., Fujiboyashi, K., Nagi, T., and Kobayashi, J. 1973. Elastic anamoly in $(NH_4)_2SO_4$ (Dielectric properties at ferroelectric transition). J. *Phys. Stat. sol. (a) 16: 279.*

Iqbal, Z., and Christoe, C. W. 1976. Raman scattering study of ferroelectric phase transition in ammonium sulphate. *solid state. Comm. 18: 269.*

Ishibashi, Y., Buchheit, W., and Peterson J. 1981. A thermodynamic potential describing the successive phase transitions in $NaNO_2$. *Solid State Comm. 38: 1277.*

Ishibashi, Y., and Shiba, H. 1978. successive phase transitions in ferroelectric $NaNO_2$ and $CS(NH_2)_2$. *J. Phys. Soc. Jap. 45: 409.*

Jain, Y. S., Bist, H. D., and Upreti, G. C. 1973. The ferroelectric phase transition in ammonium sulphate. *Chem. Phys. Lett. 22: 572.*

Kay, M. I., and Frazer, B. C. 1961. A Neutron diffraction refinement of the low temperature phase of $NaNO_2$. *Acta Crystal. 14: 56.*

Kay, M. I., Gonzalo, J. A., and Maglic, R. 1975. Phase transition in sodium nitrite. *Ferroelectrics. 9: 179.*

Klein, M. L., McDonald, I. R., and Ozaki, Y. 1982. Critical fluctuations in the paraelectric phase of $NaNO_2$. *Phys. Rev. Lett. 48: 1197.*

Komatsu, K., Itoh, K., and Nakamura E. 1988. Structural study of polarization reversal in $NaNO_2$. *J. Phys. Soc. Jap. 57: 2836.*

Laulicht, I. 1978. On the drastic temperature broadening of hard mode Raman lines of ferroelectric KDP type crystals near T_C. *J. Phys. Chem. Solids 39: 901.*

Laulicht, I., and Luknar, N. 1977. Internal-mode line-broadening by proton jumps in KH_2PO_4. *Chem. Phys. Lett. 47: 237.*

Lynden-Bell, R. M., Impey, R. W., and Klein, M. L. 1986. Investigation of the lattice vibrations of solid $NaNO_2$ by means of molecular dynamics calculations. *Chem. Phys. 109: 25*

Lynden-Bell, R. M., Klein, M. L., and McDonald, I. R. 1984. Phonon orientational coupling in sodium nitrite. *Z. Phys. B. 54:325.*

Mathias, B. T., and Remeika J. P. 1956. Ferroelectricity in ammonium sulphate. *Phys. Rev. 103: 262.*

Mitsugu, M. 1976. Anomalous temperature dependence of the frequency and damping constant of phonons near T_λ in ammonium halides. *J. Chem. Phys. 65: 1.*

Naudts, J. 1983. Mean-field theory of the incommensurate transition in $NaNO_2$. *J. Phys. C: Solid State Phys. 16: 3457*

Nordland T. J., O'Reilly D. E., and Peterson E. M. 1976. Ferroelectric mode in ammonium sulfate. *J. Chem. Phys. 64: 1838.*

Onodera, A., Cynshi, O., and Shiozaki Y. 1985. Landau theory of the ferroelectric phase transition with two order parameters. *J. Phys. C : Solid State Phys. 18: 2831.*

Onodera, A., Sugata, Y., and Shiozaki Y. 1978. Ferrielectric dielectric behaviour and the nature of phase transition of ammonioum sulphate. *Solid State. Comm. 27:243.*

O'Reilly, D. E., and Tsang, T. 1967. Deutron magnetic resonance and proton relaxation times in ferroelectric ammonium sulfate. *J. Chem. Phys. 46: 1291.*

Papon, P., Leblond, J., and Meijer, P. H. E. 2001. The physics of phase transitions. Springer- Verlag Berlin Heidelberg, Germany. P.P. 397.

Rakov, A. V. 1959. The influence of intermolecular interaction on line width in the Raman spectra of liquids. *Optics and Spectroscopy.7:128-131.*

Ramanthan, K. V., and Srinivasan, R. 1978. Proton NMR investigations of ferroelectricity in ammonium sulphate. *Chem. Phys. Lett. 56: 359.*

Ramondo, F. 1989. Structures and stabilities of $LiNO_2$ and $NaNO_2$ in pairs: An ab Initio SCF study. *Chem. Phys. Lett. 156: 346.*

Ravindran, P., Delin, A., Johansson, B., and Eriksson, O. 1999. Electronic structure, chemical bonding, and optical properties of ferroelectric and antiferroelectric $NaNO_2$. *Phys. Rev. B. 59: 1776*

Richards, R. E., and Schaefer, T. 1961. Motional narrowing and line shapes in some ammonium salts. *Trans. Faraday Soc. 57: 210.*

Rush, J. J., and Taylor, T. I. 1965. inelastic scattering of neutrons in solids and liquids. Proc. Bombay Symp., International Atomic Energy Agency, Vienna. P. 333.

Sakiyama, M., Kimato, A., and Seki, S. 1965. Heat capacities and volume thermal expansion of $NaNO_2$ crystal. *J. Phys. Soc. Jap. 20: 2180.*
Sakurai, J., Cowley, R. A., and Dolling G. J. Crystal dynamics and the ferroelectric phase transition of sodium nitrite. *J. Phys. Soc. Jap. 28: 1426.*

Sawada, S., Nomura, S., Fujii, S., and Yoshida I. 1958. Ferroelectricity in $NaNO_2$. *Phys. Rev. Lett. 1: 320.*

Sawada, A., Ohya, S., Ishibashi, Y., and Takagi, Y. 1975. Ferroelectric phase transition in $(NH_4)_2SO_4 – K_2SO_4$ mixed crystal. *J. Phys. Soc. Jap. 38: 1408.*

Sathiah, S., and Bist, H. D. 1991. Structural phase transition and internal fields in rubidium thiocyanate probed through vibrational spectroscopy. *Z. phys. B-Condensed Matter 84: 423.*

Schlemper, E. O., and Hamilton, W. C. 1966. Neutron- diffraction study of the structures of ferroelectric and paraelectric ammonium sulfate. *J. Chem. Phys. 44: 4498*

Schutte, C. J. H., and Heyns, A. 1970. Low temperature studies IV. The phase transition of ammonium sulfate and momanium- d_4 sulfate; the nature of hydrogen bonding and the reorientation of the NX_4^+ ions. *J. Chem. Phys. 52: 864.*

Shimizu, H., Ishibashi, Y., Tsukamoto, M., and Umeno, M. 1974. Brillouin scattering in sodium nitrite. *J. Phys. Soc. Jap. 36: 498.*

Syamaprasad, V., and Vallabhan, C. P. G. 1981. Observation of a high-temperature phase transition in $(NH_4)_2SO_4$ from dielectric studies. *J. Phys. C : Solid State Phys. 14: L865.*

Takagi, Y., Gesi, K. 1964. Dielectric anomalies of $NaNO_2$ above the ferroelectric curie temperature. *J. Phys. Soc. Jap. 19: 142.*

Takase, A., and Miyakawa, K. J. 1985. Temperature dependence of Raman spectra in the mixed system KNO_2- $NaNO_2$. *J. Phys. C: Solid State Phys. 18: 5579.*

Tanisaki, S. 1961. Microdomain structure in paraelectric phase of $NaNO_2$. *J. Phys. Soc. Jap. 16: 579.*

Tanisaki, S. 1961. X- ray Study on the ferroelectric phase transition of $NaNO_2$. *J. Phys. Soc. Jap. 18: 1181.*

Torrie, B. H., Lin, C. C., Binbreak, O. S., and Anderson, A. 1972. Raman and infrared studies of the ferroelectric transition in ammonium sulphate. *J. Phys. Chem. Solids 33: 697.*

Unruh, H. G. 1965. Das Curie- Weiss'sche gesetz der dielektrizitätskonstante von ammonium sulfat. *Phys. Lett. 17: 8.*

Unruh, H. G. 1970. The spontaneous polarization of $(NH_4)_2SO_4$. *Solid State. Comm. 8:1951.*

Unruh, H. G., and Ayere, O. 1976. Raman and dielectric measurements on ferroelectric ammonium sulphate. *Ferroelectrics 12: 1981.*

Vogt, H., and Happ, H. 1968. The temperature dependence of absorption of sodium nitrite in the far infrared. *Phys. Stat. Solidi. 30: 67.*

Wang, Y. X., Zhong, W. L., Wang C. L., Zhang, P. L., and Peng, Y. P. 2000. Electronic structure of $NaNO_2$ in the ferroelectric phase and paraelectric phase. *Phys. Lett. A. 269: 252.*

Watton, A., Sharp, A. R., Peton, H. G., and Pintar, M. M. 1972. Proton- magnetic-resonance study of the spin symmetry states of ammonium ions in solids. *Phys. Rev. B 5: 4281.*

Wyckoff, R. W. G. 1951. *Crystal Structures*, Interscience publishers, Inc. New York, Vol. 2, Chapter 8.

Wyncke, B., Brehat, F., Kozlov, G. V. 1984. Low-frequency dielectric response function of sodium nitrate. *Phys. Stat. Solidi (b) 129: 531.*

Yagi, T., Hikada, Y., and Miura, K. 1981. Brillouin scattering study of the incommensurate (antiferroelectric) phase in sodium nitrite. *J. De Physique, Collogue. C6: 731.*

Yagi, T., Hikada, Y., and Miura, K. 1982. Brillouin scattering study of $NaNO_2$ in the vicinity of its phase transition temperatures. *J. Phys. Soc. Jap. 51: 3562.*

Yamada, Y., Mori, M., and Noda, Y. 1972. A microscopic theory on the phase transitions in NH_4Br —an ising spin phonon coupled system— *J. Phys. Soc. Jap. 32: 1565.*

Yamada, Y., Shibuya, I. and Hoshino, S. 1963. Phase transitions in $NaNO_2$. *J. Phys. Soc. Jap. 18: 1594.*

Yamada, Y., and Yamada, T. 1966. Inter-dipolar interaction in $NaNO_2$. *J. Phys. Soc. Jap. 21: 2167.*

Yurtseven, H., and Aydogdu, A. 2001. Brillouin frequency shifts in the ferroelectric phase of $NaNO_2$. *J. Mol. Struc. 597: 31*

Yurtseven, H., and Çağlar, İ. E. 2002. Calculation of the Brillouin frequencies close to phase transitions in $NaNO_2$. *Spectrochimica Acta Part A. 58: 55.*

Yurtseven, H., Salihoğlu S., and Tari, Ö. 2001. Spontaneous polarization close to phase transitions in $NaNO_2$. *Mat. Chem. Phys. 71: 206.*